Supporting Information

Meroterpenoids from *Neosetophoma* sp.: A Dioxa[4.3.3]propellane Ring System, Potent Cytotoxicity, and Prolific Expression

Tamam El-Elimat,[†] Huzefa A. Raja,[‡] Sloan Ayers,[‡] Steven J. Kurina,[§] Joanna E. Burdette,[§] Zachary Mattes,[∥] Robert Sabatelle,[⊥] Jeffrey W. Bacon,[∥] Aaron H. Colby,[⊥] Mark W. Grinstaff,[⊥,∥] Cedric J. Pearce,[#] and Nicholas H. Oberlies*[,‡]

[†]Department of Medicinal Chemistry and Pharmacognosy, Faculty of Pharmacy, Jordan University of Science and Technology, Irbid 22110, Jordan

[‡]Department of Chemistry and Biochemistry, University of North Carolina at Greensboro, Greensboro, North Carolina 27402, United States

[§]Department of Medicinal Chemistry and Pharmacognosy, University of Illinois at Chicago, Chicago, Illinois 60612, United States

[∥]Department of Chemistry, Boston University, Boston, Massachusetts 02215, United States

[⊥]Department of Biomedical Engineering, Boston University, Boston, Massachusetts 02215, United States

[#]Mycosynthetix, Inc., Hillsborough, North Carolina 27278, United States

EXPERIMENTAL SECTION

General Experimental Procedures

Fungal Strain Isolation and Identification

Fermentation, Extraction and Isolation

Computational Details

Preparation of the (*R*)- and (*S*)-MTPA Ester Derivatives of Neosetophomone A (1) and Neosetophomone B (2)

X-ray Crystallographic Analysis of 2

Cytotoxicity Assay

Figure S1. Reversed-phase preparative HPLC chromatogram for the purification of compounds **1-6** (λ_{max} 210 nm for upper panel and λ_{max} 254 nm for lower panel). Data were acquired via a Varian Prostar HPLC system with a Phenomenex Gemini–NX C_{18} preparative (5 μm; 250 × 21.2 mm) column, and CH_3CN-H_2O (0.1% formic acid) gradient that increased linearly from 50:50 to 60:40 over 20 min at a flow rate of 21.24 mL/min.

Figure S2. UPLC chromatograms of compounds **1–6** (ELSD detection), demonstarting >97% purity. All data were acquired via an Acquity UPLC system with a BEH C_{18} (1.7 μm 2.1 × 50 mm) column and a CH_3CN–H_2O gradient that incresaed linrealy from 20 to 100 % CH_3CN over 4.5 min.

Figure S3. (+)-HRESIMS spectra of compounds **1-6**.

Table S1. ^1H (500 MHz) and ^{13}C (125 MHz) NMR data for eupenifeldin (**3**) in $CDCl_3$.

Figure S4. ^1H and ^{13}C NMR spectra of compd **3** [500 MHz for ^1H and 125 MHz for ^{13}C, $CDCl_3$].

Figure S5. COSY NMR spectrum of compd **3** [500 MHz, $CDCl_3$].

Figure S6. Edited-HSQC NMR spectrum of compd **3** [500 MHz, $CDCl_3$].

Figure S7. HMBC NMR spectrum of compd **3** [500 MHz, $CDCl_3$].

Figure S8. NOESY NMR spectrum of compd **3** [500 MHz, $CDCl_3$].

Figure S9. IR (lower frame) and VCD (upper frame) spectra observed for eupenifeldin (right axes) compared with calculated Boltzmann-averaged spectra of the calculated conformations for the 8*R*,9*S*,10*S*,12*S*,13*S* configuration, (left axes).

Figure S10. ^1H and ^{13}C NMR spectra of compd **1** [500 MHz for ^1H and 125 MHz for ^{13}C, $CDCl_3$].

Figure S11. Edited-HSQC NMR spectrum of compd **1** [500 MHz, $CDCl_3$].

Figure S12. COSY NMR spectrum of compd **1** [500 MHz, $CDCl_3$].

Figure S13. HMBC NMR spectrum of compd **1** [500 MHz, $CDCl_3$].

Figure S14. NOESY NMR spectrum of compd **1** [500 MHz, $CDCl_3$].

Figure S15. Key NOESY correlations of **1**, **2** and **4-6**.

Table S2. ^{13}C NMR data (125 MHz) for **1** in $CDCl_3$, comparing the experimental values vs those predicted by ACD software [ACD/C+H NMR Predictor and DB 2015.2.5, Advanced Chemistry Development, Inc. (Toronto, Canada)].

Figure S16. ^{1}H and ^{13}C NMR spectra of compd **2** [500 MHz for ^{1}H and 100 MHz for ^{13}C, $CDCl_3$].

Figure S17. Edited-HSQC NMR spectrum of compd **2** [400 MHz, $CDCl_3$].

Figure S18. COSY NMR spectrum of compd **2** [400 MHz, $CDCl_3$].

Figure S19. HMBC NMR spectrum of compd **2** [400 MHz, $CDCl_3$].

Figure S20. NOESY NMR spectrum of compd **2** [400 MHz, $CDCl_3$].

Figure S21. ^{1}H and ^{13}C NMR spectra of compd **4** [400 MHz for ^{1}H and 100 MHz for ^{13}C, $CDCl_3$].

Figure S22. COSY NMR spectra of compd **4** [400 MHz, $CDCl_3$].

Figure S23. Edited-HSQC NMR spectra of compd **4** [400 MHz, $CDCl_3$].

Figure S24. HMBC NMR spectra of compd **4** [400 MHz, $CDCl_3$].

Figure S25. ^{1}H and ^{13}C NMR spectra of compd **5** [500 MHz for ^{1}H and 125 MHz for ^{13}C, $CDCl_3$].

Figure S26. COSY NMR spectrum of compd **5** [500 MHz, $CDCl_3$].

Figure S27. Edited-HSQC NMR spectrum of compd **5** [500 MHz, $CDCl_3$].

Figure S28. HMBC NMR spectrum of compd **5** [500 MHz, $CDCl_3$].

Figure S29. NOESY NMR spectrum of compd **5** [500 MHz, $CDCl_3$].

Figure S30. ^{1}H and ^{13}C NMR spectra of compd **6** [500 MHz for ^{1}H and 125 MHz for ^{13}C, Methanol-d_5].

Figure S31. COSY NMR spectrum of compd **6** [400 MHz, Methanol-d_5].

Figure S32. Edited-HSQC NMR spectrum of compd **6** [400 MHz, Methanol-d_5].

Figure S33. HMBC NMR spectrum of compd **6** [400 MHz, Methanol-d_5].

Figure S34. NOESY NMR spectrum of compd **6** [500 MHz, Methanol-d_5].

Figure S35. UV spectra of compounds **1, 2, 4-6** in MeOH.

Figure S36. IR spectra of compounds **1, 2, 4-6**.

Figure S37. Phylogram of the most likely tree (-lnL = 7011.32) from a PHYML analysis of 84 taxa based on LSU sequence data (2265 bp). Numbers refer to PHYML bootstrap support values ≥ 70% based on 1000 replicates. Strain MSX50044 is identified as *Neosetophoma* sp. (Box highlighted in yellow) as it groups with other *Neosetophoma* spp. described previously. A 3-week old culture on Malt Extract agar media is shown. Bar indicates nucleotide substitutions per site.

Figure S38. Phylogram of the most likely tree (-lnL = 2946.62) from a PHYML analysis of 14 taxa based on combined ITS and LSU sequence data (1416 bp). Numbers refer to PHYML bootstrap support values ≥ 70% based on 1000 replicates. Strain MSX50044 is identified as *Neosetophoma* sp. (Box highlighted in gray) as it groups with other *Neosetophoma* spp., including type strain *N. samarorum* (CBS 138.96). Bar indicates nucleotide substitutions per site.

REFERENCES

■ EXPERIMENTAL SECTION

General Experimental Procedures. Optical rotations, UV, and IR data were measured using a Rudolph Research Autopol III polarimeter (Rudolph Research Analytical), a Varian Cary 100 Bio UV–Vis spectrophotometer (Varian Inc.), and a Perkin-Elmer Spectrum One with Universal ATR attachment (PerkinElmer). NMR spectra were recorded using a JEOL ECA–500 NMR spectrometer operating at 500 MHz for ^{1}H and 125 MHz for ^{13}C or a JEOL ECS-400 NMR spectrometer operating at 400 MHz for ^{1}H and 100 MHz for ^{13}C and equipped with a high sensitivity JEOL Royal probe and a 24-slot autosampler (both from JEOL Ltd.). Residual solvent signals were utilized for referencing. HRMS data were collected using a Thermo LTQ Orbitrap XL mass spectrometer equipped with an electrospray ionization source (Thermo Fisher Scientific). A Waters Acquity UPLC system (Waters Corp.) utilizing a Waters BEH C_{18} column (1.7 μm; 50 × 2.1 mm) was used to evaluate the purity of the isolated compounds with data collected and analyzed using Empower 3 software. Phenomenex Gemini–NX C_{18} analytical (5 μm; 250 × 4.6 mm) and preparative (5 μm; 250 × 21.2 mm) columns (all from Phenomenex) were used on a Varian Prostar HPLC system equipped with ProStar 210 pumps and a Prostar 335 photodiode array detector (PDA), with data collected and analyzed using Galaxie Chromatography Workstation software (version 1.9.3.2, Varian Inc.). Flash chromatography was performed on a Teledyne ISCO CombiFlash Rf 200 using Silica Gold columns (both from Teledyne Isco) and monitored by UV and evaporative light–scattering detectors. The IR and VCD measurements were performed on a BioTools ChiralIR FT-VCD spectrometer equipped with dual photoelastic modulation (PEM). A sample of 3.35 mg of **3** was dissolved in 150 μL $CDCl_3$ and placed in a BaF_2 cell with a path length of 100 μm, and data were acquired at 4 cm^{-1} resolution with total measurement time of 6 h and 1400 cm^{-1} PEM setting. Single-crystal X-ray diffraction data were collected using a Bruker X8 Proteum-R diffractometer (Cu Kα radiation) (Bruker Analytical X-ray Instruments Inc.). The molecular graphics were generated using Olex2 (OlexSys Ltd).

Fungal Strain Isolation and Identification. For identification of MSX50044, the nuc rDNA internal transcribed spacer rDNA region (ITS1- 5.8S-ITS2) as well as partial 28S rDNA, LSU regions were sequenced. Portions of ITS region was used for DNA barcoding, whereas, the ITS and partial LSU portion was used for evaluation of phylogenetic relationships to assess the taxonomic and phylogenetic affiliation of strain MSX50044 with the 11 previously described strains.[1-5] Methodology for DNA extraction, PCR amplification using ribosomal primers, Sanger sequencing, and Maximum Likelihood (ML) analysis have been outlined previously.[6-10] BLAST search with RefSeq database in GenBank excluding the uncultured/environmental sequences revealed *Neosetophoma* as having high sequence similarity with MSX50044. Sequences of LSU region were downloaded from recent taxonomic studies of the *Neosetophoma*[11-13] for further identification of strain MSX50044. The ML analysis using partial LSU data showed that strain MSX50044 was nested in the Phaeosphaeriaceae in a clade containing previously described *Neosetophoma* spp., including the type species, *N. samarorum,* but without significant bootstrap support (Figure S37). Further, the top matches in the ITS Refseq BLAST search: *N. rosarum, N. samarorum, N. rosigena, N. lunariae, N. clematidis, N. xingrensi,* and *N. guiyangensis* as well as sequences from the ITS region of other recently described species of *Neosetophoma* not in the RefSeq database were include from the literature in the Maximum Likelihood analysis. Results of the ML analysis using combined ITS and LSU data from type strains of eight *Neosetophoma* spp. revealed that MSX50044 could be a putative new *Neosetophoma* sp. (Figure S38). At this time and pending further investigations on the morphological characteristics of strain MSX50044, we herein refer to strain as *Neosetophoma* sp. (Ascomycota; Pezizomycotina; Dothideomycetes; Pleosporomycetidae; Pleosporales; Pleosporineae; Phaeosphaeriaceae). The sequences obtained in this study were deposited in GenBank (ITS: MK049878, MK049879; LSU: MK049274, MK049275).

Fermentation, Extraction and Isolation. Storage conditions, fermentation, and extraction procedures were as described previously.[14-16] Briefly, cultures of strain MSX50044 were grown in two separate 2.8-L Fernbach flasks (Corning, Inc., Corning, NY, USA) containing 150 g rice and 300 mL H_2O. A seed culture grown in YESD medium was used as the inoculum. Following incubation at 22 °C for 14 d, each solid culture was extracted by adding a 500 mL mixture of 1:1 MeOH-$CHCl_3$. Each culture was cut into small pieces using a spatula and shaken for about 16 h at ~125 rpm at rt, followed by vacuum filtration. The remaining residues were washed with 100 mL of 1:1 MeOH-$CHCl_3$. To the filtrate, 900 mL $CHCl_3$ and 1500 mL H_2O were added; the mixture was stirred for 30 min and then transferred into a separatory funnel. The bottom layer was drawn off and evaporated to dryness. The dried organic extracts were combined and re-constituted in 200 mL of 1:1 MeOH-CH_3CN and 200 mL of hexanes. The biphasic solution was shaken vigorously and then transferred to a separatory funnel. The MeOH-CH_3CN layer was drawn off and evaporated to dryness under vacuum. The organic defatted extract of two large scales solid culture (6.4 g) was dissolved in $CHCl_3$, adsorbed onto Celite 545, and fractionated via normal-phase flash chromatography using a gradient solvent system of hexane-$CHCl_3$-MeOH at a 85 mL/min flow rate and 25.0 column volumes over 56.5 min to afford eight fractions. About 600 mg of fraction 7 (3.5 g) was subjected to preparative HPLC over a Phenomenex Gemini–NX C_{18} preparative column using a gradient system of 50:50 to 60:40 of CH_3CN-H_2O (0.1% formic acid) over 20 min at a flow rate of 21.24 mL/min to yield 4 sub-fractions. HPLC sub-fractions 1-4 yielded compounds **1** (3.94 mg), **6** (4.96 mg), **3** (296.95 mg), and **5** (10.75 mg), which eluted at ~13.9, 17.2, 20.0, and 29.1 min, respectively (Figure S1, Supporting Information). Preparative HPLC purification of ISCO fraction **6** (276 mg) utilizing the same chromatographic conditions for fraction 7 yielded compounds **2** (56.38 mg) and **4** (6.54 mg), which eluted at ~16.2 and 40.5 min, respectively (Figure S1, Supporting Information).

Computational Details. A conformational search for the proposed absolute configuration (8*R*,9*S*,10*S*,12*S*,13*S*) was carried out with the ComputeVOA software (BioTools, Jupiter, FL, USA). Four conformers were selected to calculate vibrational frequencies, dipole transition moments, and rotational strengths at the DFT level (B3LYP functional/ 6-31G(d) basis set) with Gaussian 09 (Gaussian Inc., Wallingford, CT). The IR and VCD spectra were obtained as the sum of Lorentzian bands with a half-width of 4 cm−1. The final spectra were obtained considering the Boltzmann weighted IR and VCD spectra of each conformer. Comparison of calculated and experimental spectra was done with the CompareVOA software.

Preparation of the (*R*)- and (*S*)-MTPA Ester Derivatives of Neosetophomone A (1) and Neosetophomone B (2): To 0.42 mg of compd **1** were added 400 μL of pyridine-d_5, and the solution was transferred into an NMR tube. To initiate the reaction, 20 μL of (*R*)-(–)-α-MTPA chloride were added with careful shaking and then monitored immediately by ^{1}H NMR at the following time points: 0, 5, 10, 15, and 30 min. The reaction was found to be complete in 10 min, yielding the mono (*S*)-MTPA ester derivative (**1a**). ^{1}H NMR data of **1a** (500 MHz, pyridine-d_5): δ_H 1.62 (1H, m, H-3a), 2.15 (1H, m, H-3b), 1.93 (1H, m, H-4), 1.84 (3H, m, H$_3$-20). In an analogous manner, 0.42 mg of compd **1** dissolved in 400 μL pyridine-d_5 was reacted in a second NMR tube with 20 μL of *S*-(+)-α-methoxy-α-(trifluoromethyl)phenylacetyl (MTPA) chloride for 30 min, to afford the mono (*R*)-MTPA ester (**1b**). ^{1}H NMR data of **1b** (500 MHz, pyridine-d_5): δ_H 1.67 (1H, m, H-3a), 2.22 (1H, m, H-3b), 1.98 (1H, m, H-4), 1.63 (3H, m, H$_3$-20). In analogues manner to that of **1**, about 0.5 mg of **2** were used to prepare (*S*)- (**2a**) and (*R*)-MTPA (**2b**) ester derivatives. ^{1}H NMR data of **2a** (500 MHz, pyridine-d_5): δ_H 1.81 (3H, s, H$_3$-20), 0.97 (3H, s, H$_3$-21), 2.18 (3H, s, H$_3$-24). ^{1}H NMR data of **2b** (500 MHz, pyridine-d_5): δ_H 1.65 (3H, s, H$_3$-20), 0.95 (3H, s, H$_3$-21), 2.20 (3H, s, H$_3$-24).

*Neosetophomone A (**1**)*. White, amorphous powder; $[\alpha]_D^{20}$= –106.1° (*c* = 0.049, Chloroform) UV (MeOH) λ_{max} (log ε) 328 (2.89), 254 (3.47), 220 (3.36) nm; IR (diamond) ν_{max} 3404, 2924, 1708, 1649, 1624, 1586, 1441, 1383, 1165, 1.95, 976, 881 cm^{-1}; ^{1}H NMR ($CDCl_3$, 500 MHz) and ^{13}C NMR ($CDCl_3$, 125 MHz) (see Table 1); HRESIMS *m*/*z* 401.2315 $[M + H]^+$ (calcd. for $C_{24}H_{33}O_5$, 401.2323).

*Neosetophomone B (**2**)*. White, amorphous powder; $[\alpha]_D^{20}$= +50.0° (*c* = 0.088, Chloroform); UV (MeOH) λ_{max} (log ε) 360 (3.81), 256 (4.03) nm; IR (diamond) ν_{max} 3396, 2950, 1590, 1525, 1438, 1380, 1280, 1153, 1129, 1080, 1044, 988, 894 cm^{-1}; ^{1}H NMR ($CDCl_3$, 500 MHz) and ^{13}C NMR ($CDCl_3$, 100 MHz) (see Table 2); HRESIMS *m*/*z* 385.2368 $[M + H]^+$ (calcd. for $C_{24}H_{33}O_4$, 385.2373).

*Eupenifeldin (**3**)*. White, amorphous powder; $[\alpha]_D^{20}$= +223.2° (*c* = 0.056, Chloroform); ^{1}H NMR ($CDCl_3$, 500 MHz) and ^{13}C NMR ($CDCl_3$, 125 MHz) (see Table S1, Supporting Information); HRESIMS *m*/*z* 549.2828 $[M + H]^+$ (calcd. for $C_{33}H_{41}O_7$, 549.2847).

*Dehydroxynoreupenifeldin (**4**)*. White, amorphous powder; $[\alpha]_D^{20}$= +223.5° (*c* = 0.017, Methanol); UV (MeOH) λ_{max} (log ε) 360 (3.85), 257 (4.04) nm; IR (diamond) ν_{max} 2927, 1590, 1439, 1374, 1280, 1168, 1083, 1044, 895, 721 cm^{-1}; ^{1}H NMR ($CDCl_3$, 500 MHz) and ^{13}C NMR ($CDCl_3$, 125 MHz) (see Tables 3 and 4); HRESIMS *m*/*z* 533.2885 $[M + H]^+$ (calcd. for $C_{33}H_{41}O_6$, 533.2898).

*Noreupenifeldin B (**5**)*. White, amorphous powder; $[\alpha]_D^{20}$= +132.7° (*c* = 0.049, Chloroform); UV (MeOH) λ_{max} (log ε) 366 (3.55), 259 (3.60) nm; IR (diamond) ν_{max} 3260, 2925, 1620, 1588, 1464, 1422, 1292, 1140, 1084, 1027, 983, 899, 842 cm^{-1}; ^{1}H NMR ($CDCl_3$, 500 MHz) and ^{13}C NMR ($CDCl_3$, 125 MHz) (see Tables 3 and 4); HRESIMS *m*/*z* 521.2879 $[M + H]^+$ (calcd. for $C_{32}H_{41}O_6$, 521.2898).

*22-Hydroxyramiferin (**6**)*. Light brown, amorphous powder; $[\alpha]_D^{20}$= +88.9° (*c* = 0.054, Chloroform); UV (MeOH) λ_{max} (log ε) 366 (3.00), 271 (3.42), 259 (3.41), 230 (3.50) nm; IR (diamond) ν_{max} 3303, 2926, 1593, 1463, 1366, 1319, 1138, 1085, 992, 838 cm^{-1}; ^{1}H NMR (methanol-d_4, 500 MHz) and ^{13}C NMR

(methanol-d_4, 125 MHz) (see Tables 3 and 4); HRESIMS *m*/*z* 509.2878 $[M + H]^+$ (calcd. for $C_{31}H_{41}O_6$, 509.2898).

X-ray Crystallographic Analysis of 2. Crystals of **2** were grown in a mixture of MeCN and chloroform at rt.

Computing Details. Data collection: X8 Proteum-R (Bruker Analytical X-ray Instruments Inc., Madison, Wisconsin, USA); cell refinement: SAINT V8.38A (Bruker Analytical X-ray Instruments Inc., Madison, Wisconsin, USA); data reduction: SAINT V8.38A (Bruker Analytical X-ray Instruments Inc., Madison, Wisconsin, USA); program(s) used to solve structure: ShelXT;[17] program(s) used to refine structure: SHELXL;[17] molecular graphics: Olex2 (Dolomanov et al., 2009);[18] software used to prepare material for publication: Olex2.[18] publCIF is used for generating the crystallographic information file (CIF).[19]

Crystal Data

$C_{24}H_{32}O_4 \cdot H_2O$	D_x = 1.240 Mg m^{-3}
M_r = 402.51	Cu $K\alpha$ radiation, λ = 1.54178 Å
Orthorhombic, $P2_12_12_1$	Cell parameters from 9817 reflections
a = 8.3102 (3) Å	θ = 4.0–66.5°
b = 13.8111 (5) Å	μ = 0.69 mm^{-1}
c = 18.7895 (7) Å	*T* = 100 K
V = 2156.53 (14) Å^3	Plate, colourless
Z = 4	0.14 × 0.12 × 0.03 mm
F(000) = 872	

Data Collection

Bruker X8 Proteum-R diffractometer	3807 independent reflections
Radiation source: rotating anode	3672 reflections with $I > 2\sigma(I)$
Montel monochromator	R_{int} = 0.051
ϕ and ω scans	θ_{max} = 66.7°, θ_{min} = 4.0°
Absorption correction: multi-scan *SADABS2016*/2 (Bruker,2016/2) was used for absorption correction. wR2(int) was 0.0786 before and 0.0656 after correction. The Ratio of minimum to maximum transmission is 0.8746.	*h* = -9→9

The λ/2 correction factor is Not present.	
T_{min} = 0.658, T_{max} = 0.753	k = -14→16
53741 measured reflections	l = -22→21

Refinement

Refinement on F^2	Secondary atom site location: difference Fourier map
Least-squares matrix: full	Hydrogen site location: mixed
$R[F^2 > 2\sigma(F^2)]$ = 0.025	H atoms treated by a mixture of independent and constrained refinement
$wR(F^2)$ = 0.061	$w = 1/[\sigma^2(F_o^2) + (0.022P)^2 + 0.5187P]$ where $P = (F_o^2 + 2F_c^2)/3$
S = 1.10	$(\Delta/\sigma)_{max} < 0.001$
3807 reflections	$\Delta\rangle_{max}$ = 0.13 e Å^{-3}
279 parameters	$\Delta\rangle_{min}$ = -0.11 e Å^{-3}
0 restraints	Absolute structure: Flack x determined using 1535 quotients [(I+)-(I-)]/[(I+)+(I-)] (Parsons, Flack and Wagner, Acta Cryst. B69 (2013) 249-259).
Primary atom site location: dual	Absolute structure parameter: 0.10 (4)

Special Details

Geometry. All esds (except the esd in the dihedral angle between two l.s. planes) were estimated using the full covariance matrix. The cell esds are taken into account individually in the estimation of esds in distances, angles and torsion angles; correlations between esds in cell parameters are only used when they are defined by crystal symmetry. An approximate (isotropic) treatment of cell esds is used for estimating esds involving l.s. planes.

Fractional Atomic Coordinates and Isotropic or Equivalent Isotropic Displacement Parameters (Å^2)

	x	y	z	U_{iso}*/U_{eq}
O4	0.43539 (15)	0.38097 (9)	0.59320 (6)	0.0188 (3)
H4	0.504 (3)	0.3343 (17)	0.6084 (12)	0.028*
O3	0.80321 (14)	0.58023 (9)	0.35101 (6)	0.0194 (3)

O2	0.82103 (15)	0.74679 (9)	0.14476 (7)	0.0209 (3)
H2	0.771 (3)	0.7608 (17)	0.1008 (13)	0.031*
O1W	0.81011 (18)	0.81143 (10)	0.01001 (7)	0.0292 (3)
H1WA	0.897 (3)	0.8022 (19)	-0.0228 (14)	0.044*
O1	0.54804 (17)	0.71162 (11)	0.08735 (7)	0.0348 (4)
C16	0.7185 (2)	0.69111 (12)	0.18240 (9)	0.0162 (3)
C7	0.8609 (2)	0.60447 (14)	0.50587 (9)	0.0194 (4)
H7	0.836822	0.665151	0.484588	0.023*
C15	0.7710 (2)	0.65675 (13)	0.24590 (9)	0.0175 (4)
H15	0.876179	0.677452	0.258507	0.021*
C2	0.53175 (19)	0.45749 (12)	0.56106 (9)	0.0146 (3)
H2A	0.638798	0.460748	0.585252	0.018*
C1	0.4417 (2)	0.55096 (12)	0.57332 (9)	0.0159 (3)
C17	0.5641 (2)	0.67369 (13)	0.14781 (9)	0.0193 (4)
C14	0.6967 (2)	0.59526 (13)	0.29706 (8)	0.0157 (3)
C13	0.5432 (2)	0.55565 (12)	0.29785 (8)	0.0149 (3)
C3	0.5555 (2)	0.42908 (13)	0.48248 (9)	0.0187 (4)
H3A	0.453508	0.399597	0.465984	0.022*
H3B	0.638051	0.377427	0.481222	0.022*
C12	0.4947 (2)	0.49552 (13)	0.36171 (9)	0.0167 (3)
H12A	0.492387	0.426554	0.347389	0.020*
H12B	0.384044	0.513913	0.375750	0.020*
C8	0.8548 (2)	0.59680 (13)	0.57586 (9)	0.0178 (4)
H8	0.893876	0.537571	0.594897	0.021*
C24	0.2676 (2)	0.51468 (14)	0.25195 (9)	0.0221 (4)
H24A	0.286990	0.445889	0.261444	0.033*
H24B	0.202749	0.521419	0.208682	0.033*
H24C	0.210036	0.543502	0.292230	0.033*
C18	0.4396 (2)	0.61711 (13)	0.17868 (9)	0.0181 (4)
H18	0.345417	0.613476	0.150141	0.022*
C5	0.7795 (2)	0.49985 (14)	0.40115 (9)	0.0176 (4)
C4	0.60450 (19)	0.50578 (13)	0.42667 (8)	0.0146 (3)
H4A	0.586732	0.571363	0.447811	0.018*
C11	0.4933 (2)	0.62179 (13)	0.61602 (9)	0.0194 (4)
H11	0.428372	0.678411	0.616759	0.023*
C6	0.9045 (2)	0.52099 (14)	0.45883 (9)	0.0212 (4)
H6A	0.918194	0.462451	0.488625	0.025*

H6B	1.009110	0.534784	0.435747	0.025*
C19	0.4277 (2)	0.56626 (12)	0.24185 (9)	0.0163 (3)
C9	0.7945 (2)	0.66883 (13)	0.62958 (9)	0.0205 (4)
C20	0.2794 (2)	0.55785 (14)	0.53779 (10)	0.0210 (4)
H20A	0.292782	0.553198	0.486086	0.032*
H20B	0.229336	0.619988	0.549777	0.032*
H20C	0.210625	0.504837	0.554425	0.032*
C10	0.6396 (2)	0.62454 (13)	0.66311 (9)	0.0212 (4)
H10A	0.664236	0.557533	0.678348	0.025*
H10B	0.612698	0.662079	0.706387	0.025*
C21	0.9218 (3)	0.67971 (14)	0.68822 (10)	0.0278 (4)
H21A	0.943456	0.616311	0.709606	0.042*
H21B	0.882040	0.724151	0.724873	0.042*
H21C	1.021251	0.705605	0.667624	0.042*
C23	0.8217 (2)	0.40607 (14)	0.36281 (10)	0.0254 (4)
H23A	0.753823	0.399236	0.320455	0.038*
H23B	0.803353	0.351084	0.394763	0.038*
H23C	0.935102	0.407544	0.348540	0.038*
C22	0.7580 (3)	0.76754 (14)	0.59719 (11)	0.0294 (5)
H22A	0.857184	0.795514	0.577850	0.044*
H22B	0.714488	0.810486	0.633976	0.044*
H22C	0.678887	0.760121	0.558904	0.044*
H1WB	0.722 (3)	0.8206 (19)	-0.0215 (14)	0.044*

Atomic Displacement Parameters (Å^2)

	U^{11}	U^{22}	U^{33}	U^{12}	U^{13}	U^{23}
O4	0.0182 (6)	0.0182 (6)	0.0200 (6)	-0.0022 (5)	0.0001 (5)	0.0077 (5)
O3	0.0146 (6)	0.0302 (7)	0.0133 (5)	-0.0026 (5)	-0.0018 (5)	0.0053 (5)
O2	0.0205 (6)	0.0234 (7)	0.0187 (6)	-0.0007 (5)	0.0014 (5)	0.0060 (5)
O1W	0.0264 (7)	0.0373 (8)	0.0240 (7)	0.0099 (7)	0.0051 (6)	0.0081 (6)
O1	0.0317 (8)	0.0473 (9)	0.0254 (7)	-0.0096 (7)	-0.0108 (6)	0.0185 (6)
C16	0.0181 (8)	0.0145 (8)	0.0161 (8)	0.0017 (7)	0.0036 (7)	-0.0009 (7)
C7	0.0156 (8)	0.0221 (9)	0.0205 (9)	-0.0046 (7)	-0.0047 (7)	0.0059 (7)
C15	0.0137 (8)	0.0228 (9)	0.0160 (8)	-0.0001 (7)	0.0003 (7)	-0.0008 (7)
C2	0.0130 (7)	0.0167 (8)	0.0141 (8)	-0.0028 (7)	-0.0002 (6)	0.0043 (6)
C1	0.0154 (8)	0.0194 (9)	0.0130 (8)	0.0013 (7)	0.0030 (7)	0.0058 (7)

C17	0.0241 (9)	0.0190 (8)	0.0150 (8)	0.0024 (7)	-0.0025 (7)	0.0013 (7)
C14	0.0164 (8)	0.0199 (9)	0.0107 (7)	0.0032 (7)	-0.0008 (7)	-0.0022 (6)
C13	0.0167 (8)	0.0160 (8)	0.0119 (8)	0.0014 (7)	0.0011 (6)	-0.0025 (6)
C3	0.0229 (9)	0.0168 (8)	0.0165 (8)	-0.0031 (7)	0.0011 (7)	0.0005 (7)
C12	0.0166 (8)	0.0195 (8)	0.0141 (8)	-0.0024 (7)	0.0005 (7)	-0.0009 (7)
C8	0.0155 (8)	0.0186 (9)	0.0194 (9)	-0.0041 (7)	-0.0052 (7)	0.0037 (7)
C24	0.0199 (9)	0.0280 (10)	0.0183 (8)	-0.0053 (8)	-0.0045 (7)	-0.0007 (8)
C18	0.0177 (8)	0.0210 (9)	0.0156 (8)	0.0015 (7)	-0.0048 (7)	-0.0019 (7)
C5	0.0176 (9)	0.0227 (9)	0.0125 (8)	0.0009 (7)	0.0005 (7)	0.0035 (7)
C4	0.0154 (8)	0.0168 (8)	0.0117 (7)	-0.0005 (7)	0.0005 (6)	-0.0005 (7)
C11	0.0219 (9)	0.0193 (9)	0.0170 (8)	0.0036 (7)	0.0039 (7)	0.0023 (7)
C6	0.0154 (8)	0.0322 (11)	0.0158 (8)	0.0008 (7)	-0.0014 (7)	0.0041 (8)
C19	0.0169 (8)	0.0156 (8)	0.0165 (8)	0.0011 (7)	-0.0006 (7)	-0.0051 (6)
C9	0.0273 (10)	0.0159 (9)	0.0182 (8)	-0.0031 (8)	-0.0074 (8)	0.0020 (7)
C20	0.0160 (8)	0.0244 (9)	0.0226 (9)	0.0017 (7)	0.0007 (7)	0.0066 (7)
C10	0.0300 (10)	0.0192 (9)	0.0144 (8)	0.0002 (8)	-0.0013 (7)	-0.0014 (7)
C21	0.0381 (11)	0.0230 (10)	0.0223 (9)	-0.0060 (9)	-0.0126 (9)	0.0010 (8)
C23	0.0263 (10)	0.0308 (10)	0.0191 (9)	0.0089 (8)	0.0012 (7)	-0.0015 (8)
C22	0.0416 (12)	0.0165 (9)	0.0300 (10)	-0.0032 (8)	-0.0095 (9)	0.0032 (8)

Geometric parameters (Å, º)

O4—C2	1.457 (2)	C14—C13	1.388 (3)
O3—C14	1.361 (2)	C13—C12	1.514 (2)
O3—C5	1.469 (2)	C13—C19	1.432 (2)
O2—C16	1.348 (2)	C3—C4	1.545 (2)
O1—C17	1.258 (2)	C12—C4	1.530 (2)
C16—C15	1.356 (2)	C8—C9	1.503 (3)
C16—C17	1.459 (3)	C24—C19	1.521 (2)
C7—C8	1.320 (2)	C18—C19	1.383 (2)
C7—C6	1.497 (3)	C5—C4	1.533 (2)
C15—C14	1.423 (2)	C5—C6	1.530 (2)
C2—C1	1.510 (2)	C5—C23	1.523 (3)
C2—C3	1.540 (2)	C11—C10	1.505 (3)
C1—C11	1.336 (3)	C9—C10	1.558 (3)
C1—C20	1.508 (2)	C9—C21	1.535 (3)
C17—C18	1.420 (3)	C9—C22	1.524 (3)

C14—O3—C5	120.36 (13)	C7—C8—C9	128.95 (17)
O2—C16—C15	117.27 (15)	C19—C18—C17	133.01 (16)
O2—C16—C17	114.60 (14)	O3—C5—C4	106.71 (13)
C15—C16—C17	128.11 (16)	O3—C5—C6	102.64 (14)
C8—C7—C6	122.38 (17)	O3—C5—C23	107.95 (13)
C16—C15—C14	131.60 (16)	C6—C5—C4	114.36 (14)
O4—C2—C1	106.52 (13)	C23—C5—C4	114.32 (15)
O4—C2—C3	106.43 (13)	C23—C5—C6	109.93 (14)
C1—C2—C3	115.31 (14)	C12—C4—C3	108.70 (14)
C11—C1—C2	123.96 (15)	C12—C4—C5	108.11 (13)
C11—C1—C20	120.44 (16)	C5—C4—C3	115.19 (14)
C20—C1—C2	115.46 (15)	C1—C11—C10	129.13 (16)
O1—C17—C16	115.28 (16)	C7—C6—C5	113.64 (15)
O1—C17—C18	121.37 (17)	C13—C19—C24	116.54 (15)
C18—C17—C16	123.35 (15)	C18—C19—C13	129.41 (16)
O3—C14—C15	108.20 (14)	C18—C19—C24	114.05 (15)
O3—C14—C13	121.96 (15)	C8—C9—C10	106.67 (14)
C13—C14—C15	129.83 (15)	C8—C9—C21	108.50 (16)
C14—C13—C12	117.98 (15)	C8—C9—C22	112.98 (15)
C14—C13—C19	124.61 (15)	C21—C9—C10	108.51 (15)
C19—C13—C12	117.40 (15)	C22—C9—C10	110.38 (16)
C2—C3—C4	120.63 (14)	C22—C9—C21	109.66 (15)
C13—C12—C4	115.01 (14)	C11—C10—C9	116.10 (14)

Cytotoxicity Assay. The initial screening of the cultures against NCI-H460[20] human large cell lung carcinoma (HTB-177, American Type Culture Collection (ATCC) was carried out as described previously.[21,22] For the pure compound testing, human breast, ovarian mesothelioma, lung and murine lung cancer cells designated MDA–MB–231, OVCAR 3, OVCAR 8, MSTO-211H, A549 and LLC respectively, were purchased from the American Type Culture Collection (Manassas, VA). The cell lines were propagated at 37 °C in 5% CO_2 in RPMI 1640 medium or F12K (A549) or Dulbecco's Modified Eagle's Medium (LLC) supplemented with fetal bovine serum (10%), penicillin (100 units/mL), and streptomycin (100 μg/mL). Cells in log phase growth were harvested by trypsinization followed by two

washings to remove all traces of enzyme. A total of 5,000 cells were seeded per well of a 96-well clear, flat-bottom plate (Microtest 96, Falcon) and incubated overnight (37 °C in 5% CO_2). Samples dissolved in DMSO were then diluted and added to the appropriate wells. The cells were incubated in the presence of test substance for 72 h at 37 °C and evaluated for viability with a commercial absorbance assay (CellTiter-Blue Cell Viability Assay, Promega Corp, Madison, WI or MTT Cell Proliferation Assay, ATCC, Manassas, VA) that measured viable cells. IC_{50} values are expressed in μM relative to the solvent (DMSO) control.

Mitochondrial Toxicity Assay. Mitochondrial toxicity was evaluated using a Promega Mitochondrial ToxGlo™ kit. Human hepatocellular carcinoma cells (HepG2) and human glioblastoma cells (U-87MG) were cultured in standard growth conditions (Dulbecco's modified Eagle's medium with 10% FBS, 100 U/mL penicillin and streptomycin) at 37 °C and 5% CO_2. Cells were seeded at a density of 10,000 cells/well in 96 well tissue culture plates in either glucose (25 mM) or galactose (10 mM) supplemented media and were incubated for 8 hours to allow for cell adherence. The Mitochondrial ToxGlo™ assay was performed in accordance with manufacturer instructions. Cells were incubated with test compounds for 90 minutes prior to assay per the manufacturer's protocol. Cells were incubated for 30 minutes with a cell impermeable, fluorogenic substrate, and fluorescence (Ex/Em 485/525 nm) was measured. Lysis buffer was then added and net ATP levels were determined by luminescence measurement from a luciferase reporter. Test compounds were solubilized in DMSO prior to assay and the assay was run at a .5% DMSO final media concentration.

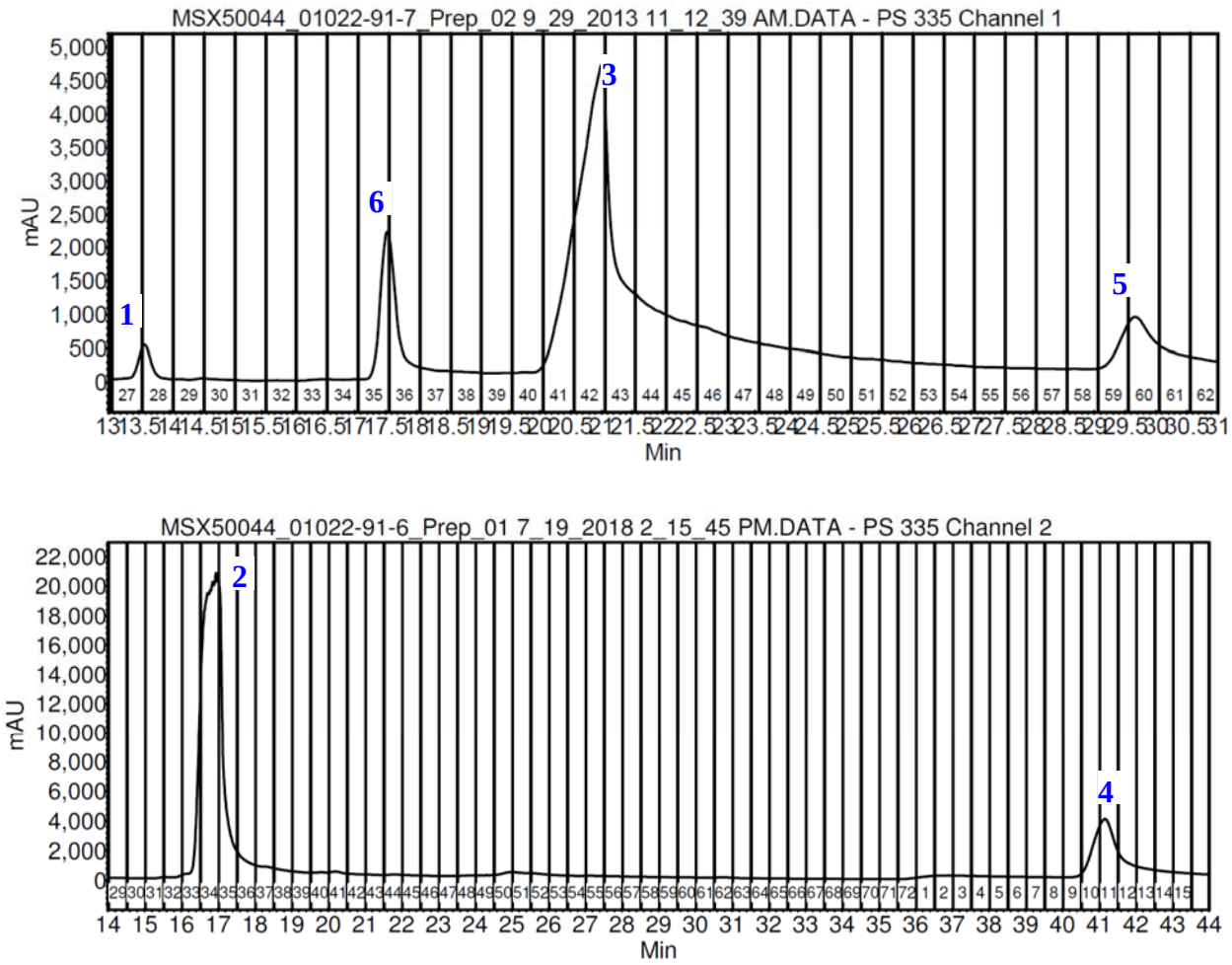

Figure S1. Reversed-phase preparative HPLC chromatogram for the purification of compounds **1-6** (λ_{max} 210 nm for upper panel and λ_{max} 254 nm for lower panel). Data were acquired via a Varian Prostar HPLC system with a Phenomenex Gemini–NX C_{18} preparative (5 μm; 250 × 21.2 mm) column, and CH_3CN-H_2O (0.1% formic acid) gradient that increased linearly from 50:50 to 60:40 over 20 min at a flow rate of 21.24 mL/min.

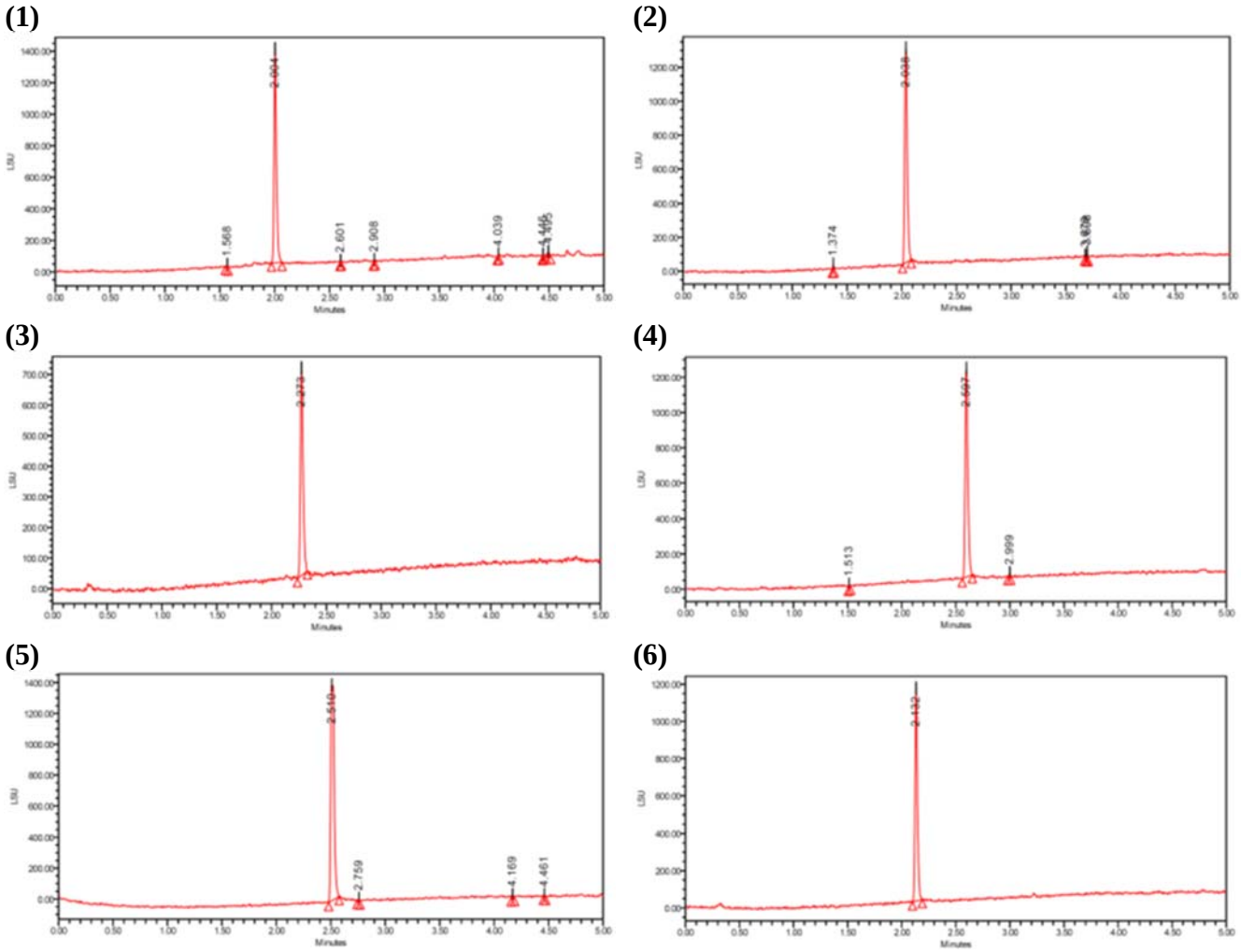

Figure S2. UPLC chromatograms of compounds **1–6** (ELSD detection), demonstarting >97% purity. All data were acquired via an Acquity UPLC system with a BEH C_{18} (1.7 μm 2.1 × 50 mm) column and a CH_3CN–H_2O gradient that incresaed linrealy from 20 to 100 % CH_3CN over 4.5 min.

Compd **1**

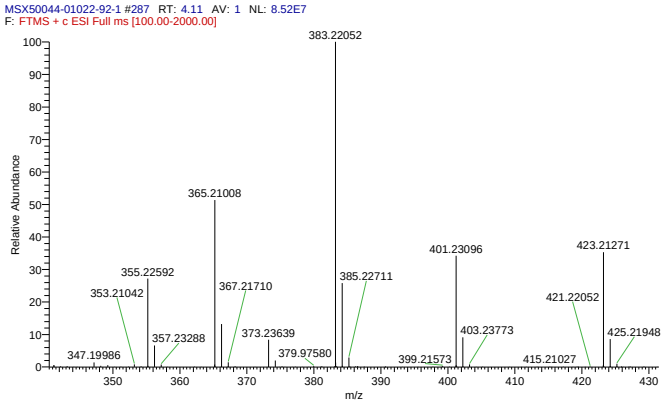

Compd **2**

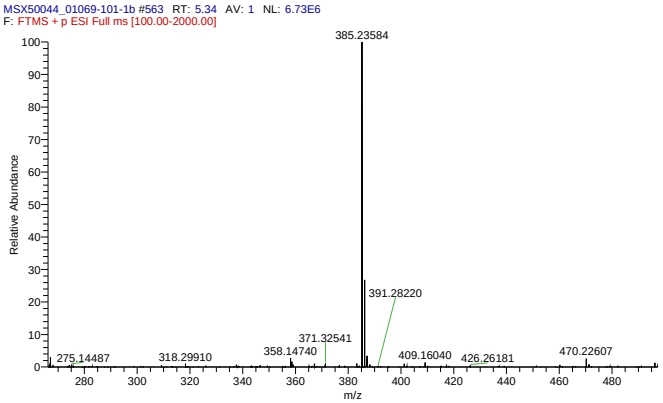

Compd **3**

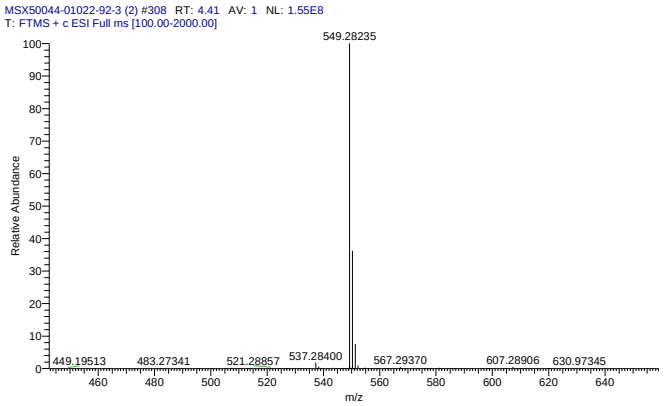

Compd **4**

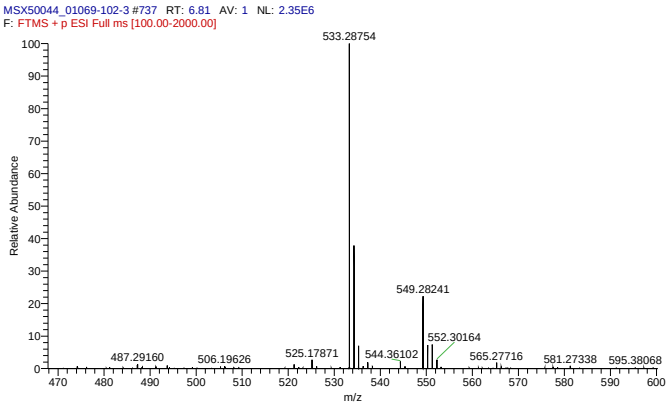

Compd **5**

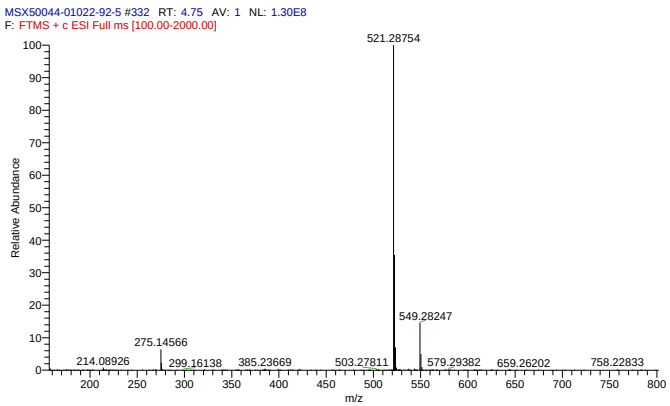

Compd **6**

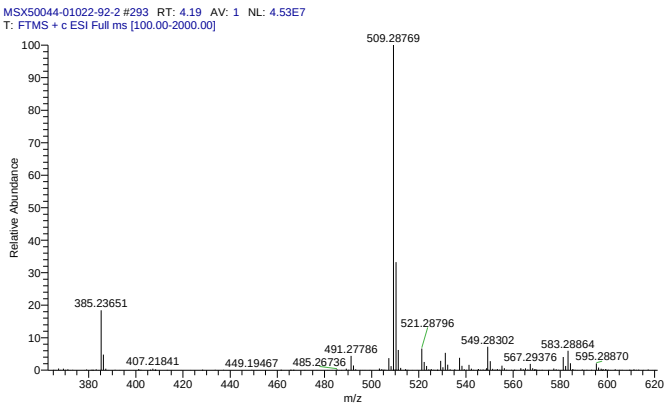

Figure S3. (+)-HRESIMS spectra of compounds **1-6**.

Table S1. ^{1}H (500 MHz) and ^{13}C (125 MHz) NMR data for eupenifeldin (**3**) in $CDCl_3$.

position	δ_C, mult	δ_H (J in Hz)
1	173.4, C	
2	162.8, C	
3	112.9, CH	6.90 (s)
4	159.6, C	
5	118.8, C	
6	151.6, C	
7	125.7, CH	7.13 (s)
8	34.4, CH_2	2.35 (m); 2.83 (dd, 17.2, 5.2)
9	32.0, CH	1.80 (m)
10	82.0, C	
11	70.8, CH	4.20 (d, 11.5)
12	30.2, CH_2	1.51 (t, 12.0); 2.19 (m)
13	41.6, CH	2.16 (m)
14	80.6, C	
15	46.3, CH_2	2.49 (dd, 13.2, 11.5); 2.71 (dd, 13.2, 4.0)
16	125.9, CH	5.66 (ddd, 16.0, 11.5, 4.0)
17	144.1, CH	5.77 (d, 16.0)
18	35.0, C	
19	46.6, CH_2	0.75 (dd, 14.3, 4.0); 1.76 (d, 14.3)
20	33.1, CH_2	2.38 (m); 3.36 (dd, 14.3, 13.8)
21	122.6, C	
22	160.4, C	
23	113.6, CH	6.92 (s)
24	163.2, C	
25	172.7, C	
26	124.8, CH	7.10 (s)
27	150.7, C	
28	27.6, CH_3	2.35 (s)
29	16.2, CH_3	1.12 (s)
30	29.8, CH_3	1.05 (s)
31	27.3, CH_3	1.08 (s)
32	19.4, CH_3	1.38 (s)
33	27.6, CH_3	2.39 (s)

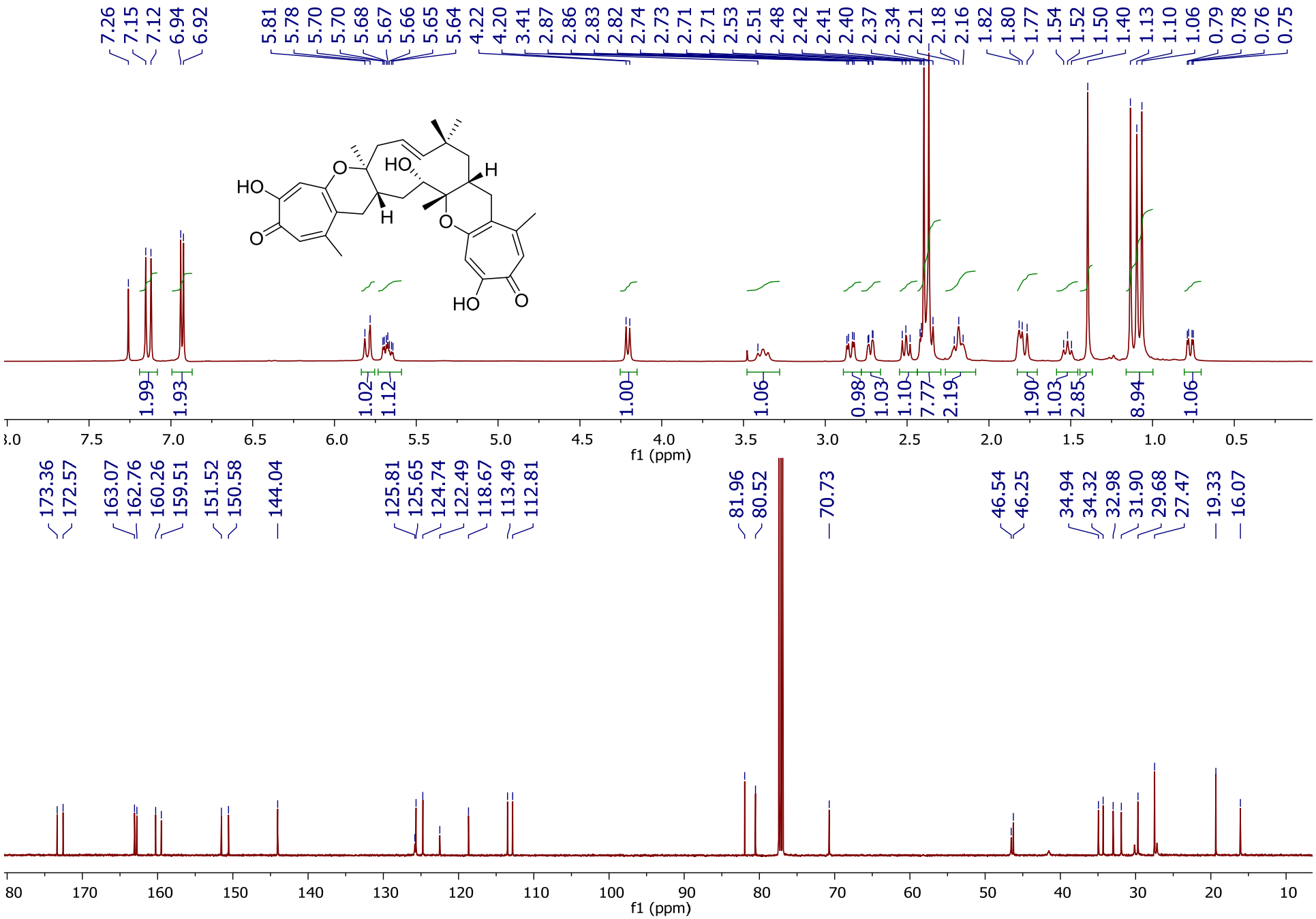

Figure S4. ^{1}H and ^{13}C NMR spectra of compd **3** [500 MHz for ^{1}H and 125 MHz for ^{13}C, $CDCl_3$].

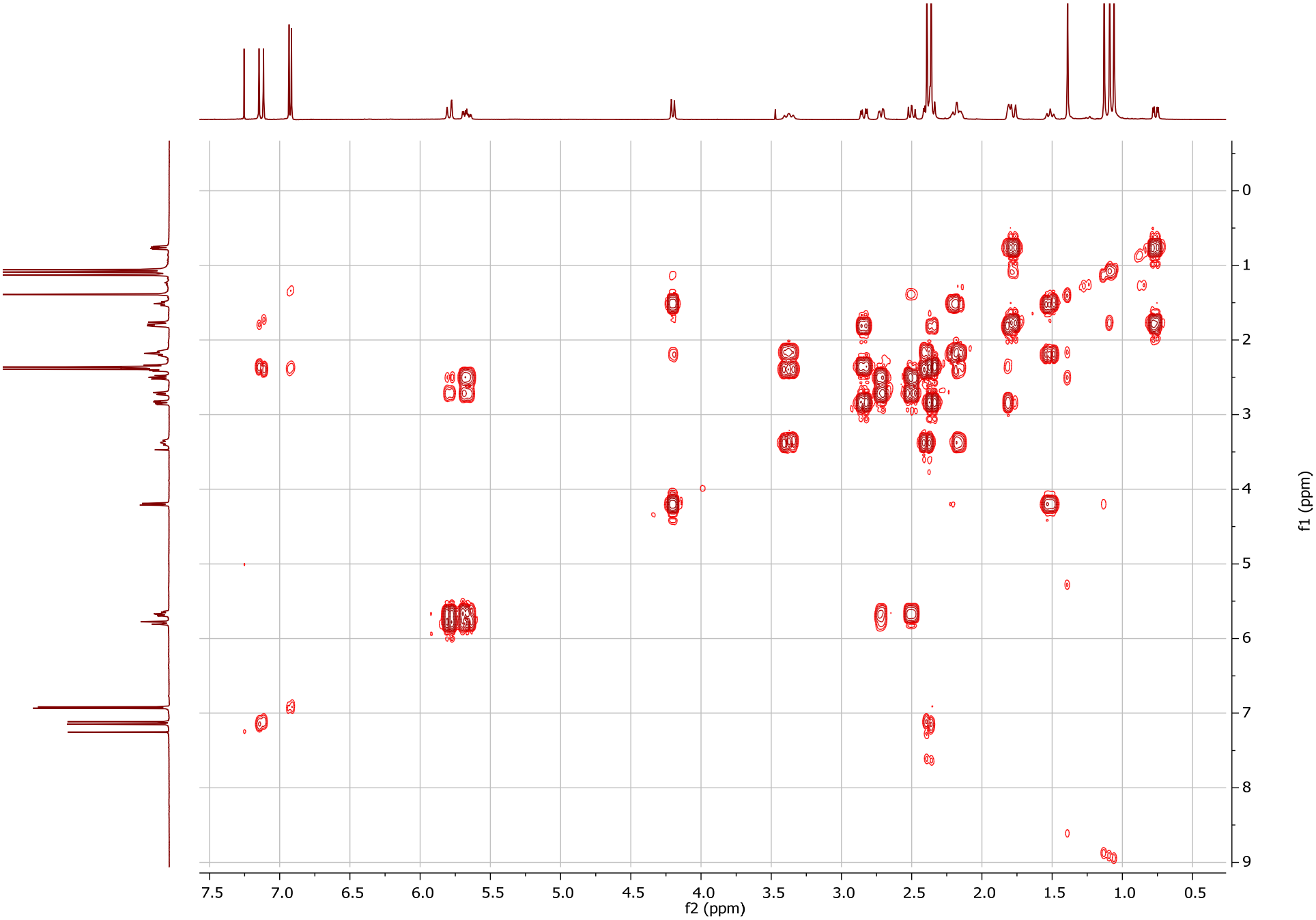

Figure S5. COSY NMR spectrum of compd **3** [500 MHz, $CDCl_3$].

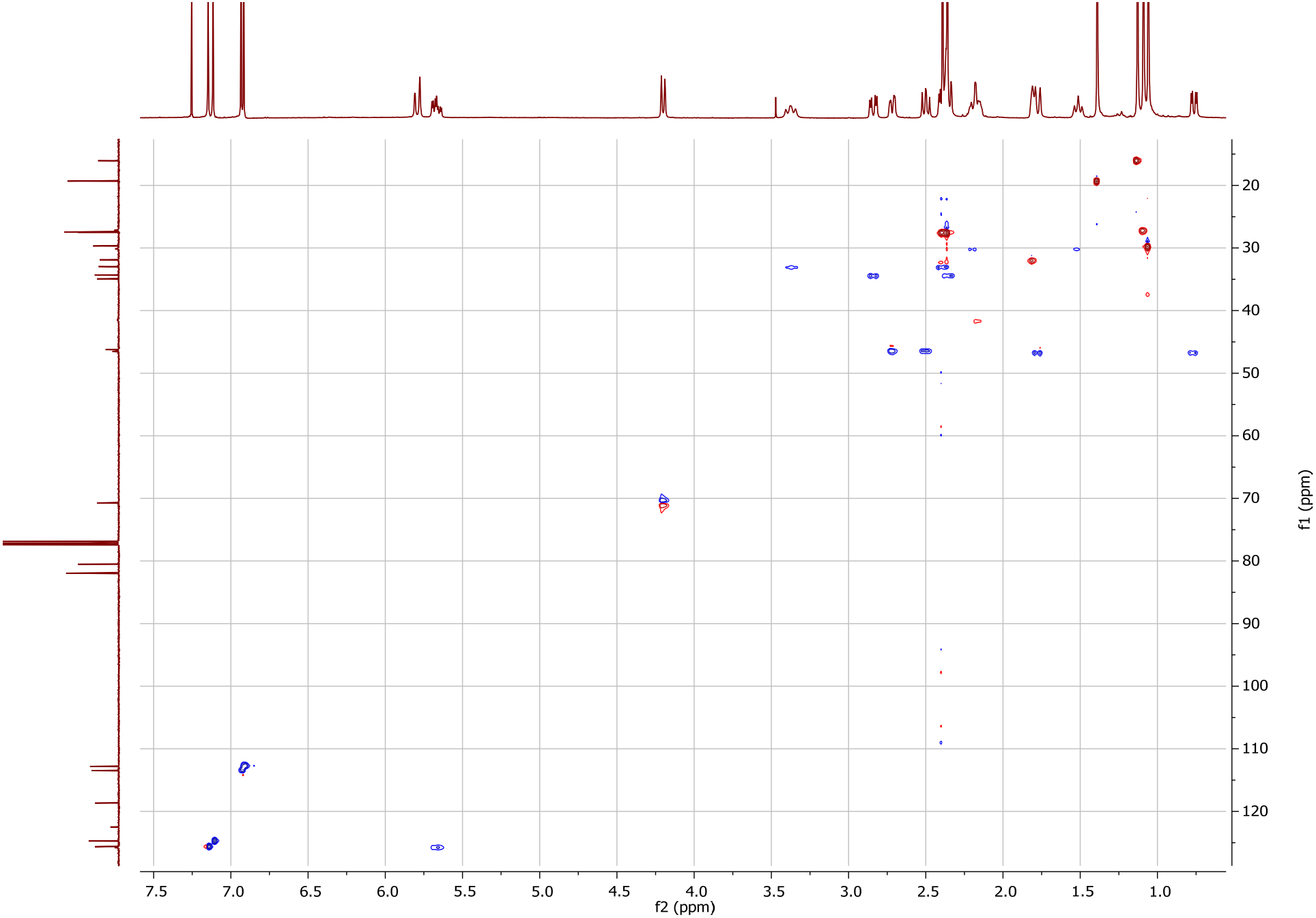

Figure S6. Edited-HSQC NMR spectrum of compd **3** [500 MHz, $CDCl_3$].

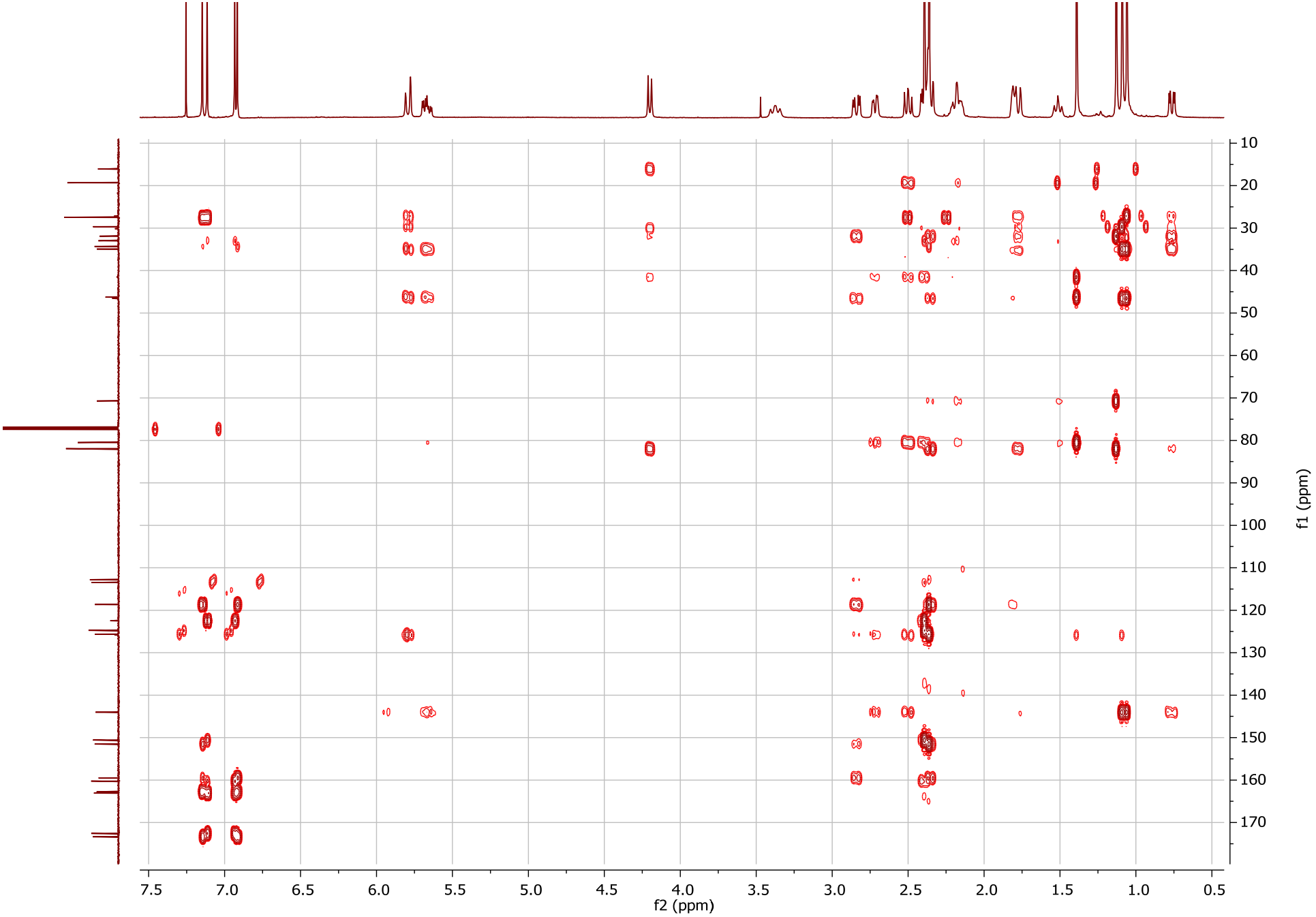

Figure S7. HMBC NMR spectrum of compd **3** [500 MHz, $CDCl_3$].

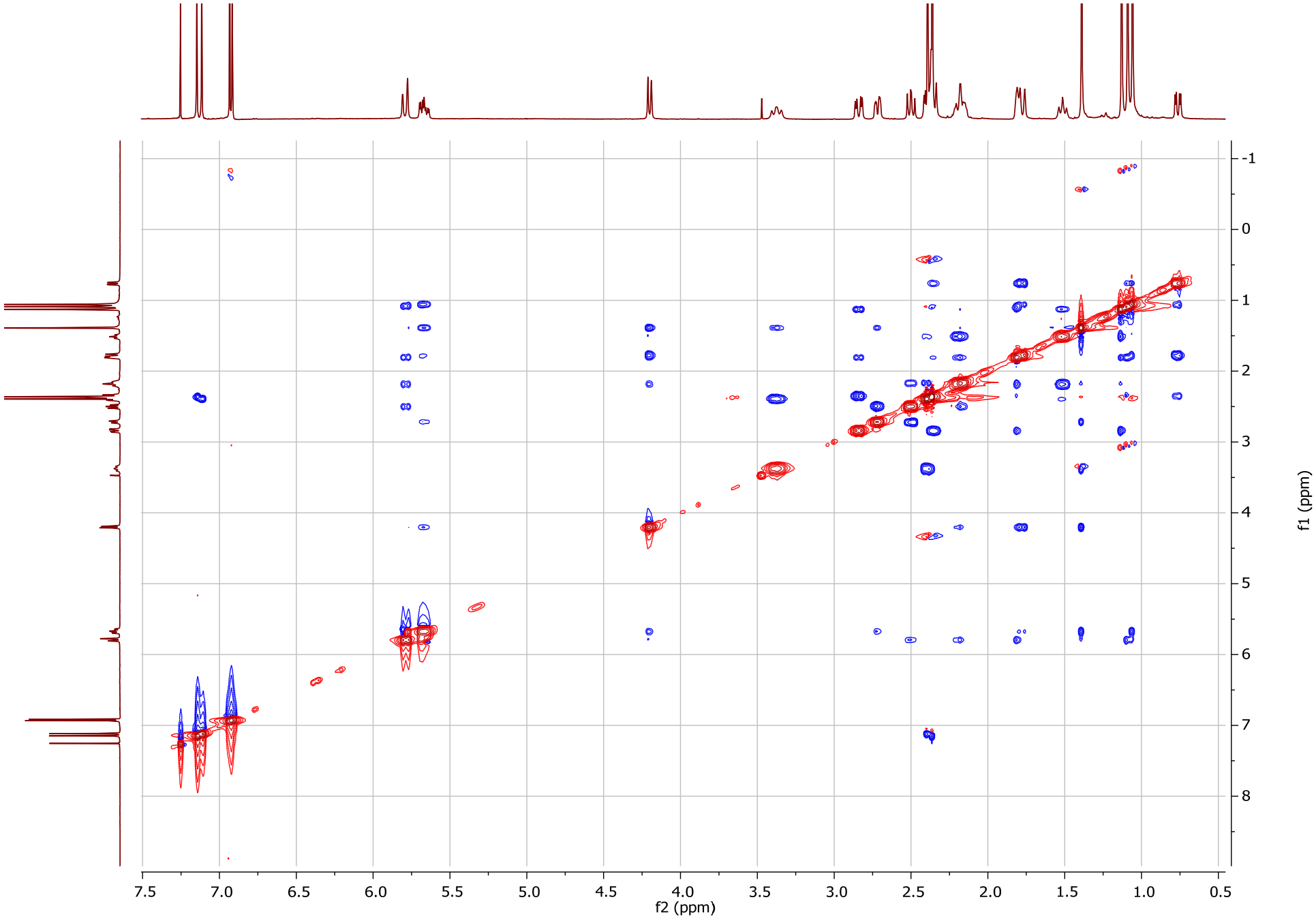

Figure S8. NOESY NMR spectrum of compd **3** [500 MHz, $CDCl_3$].

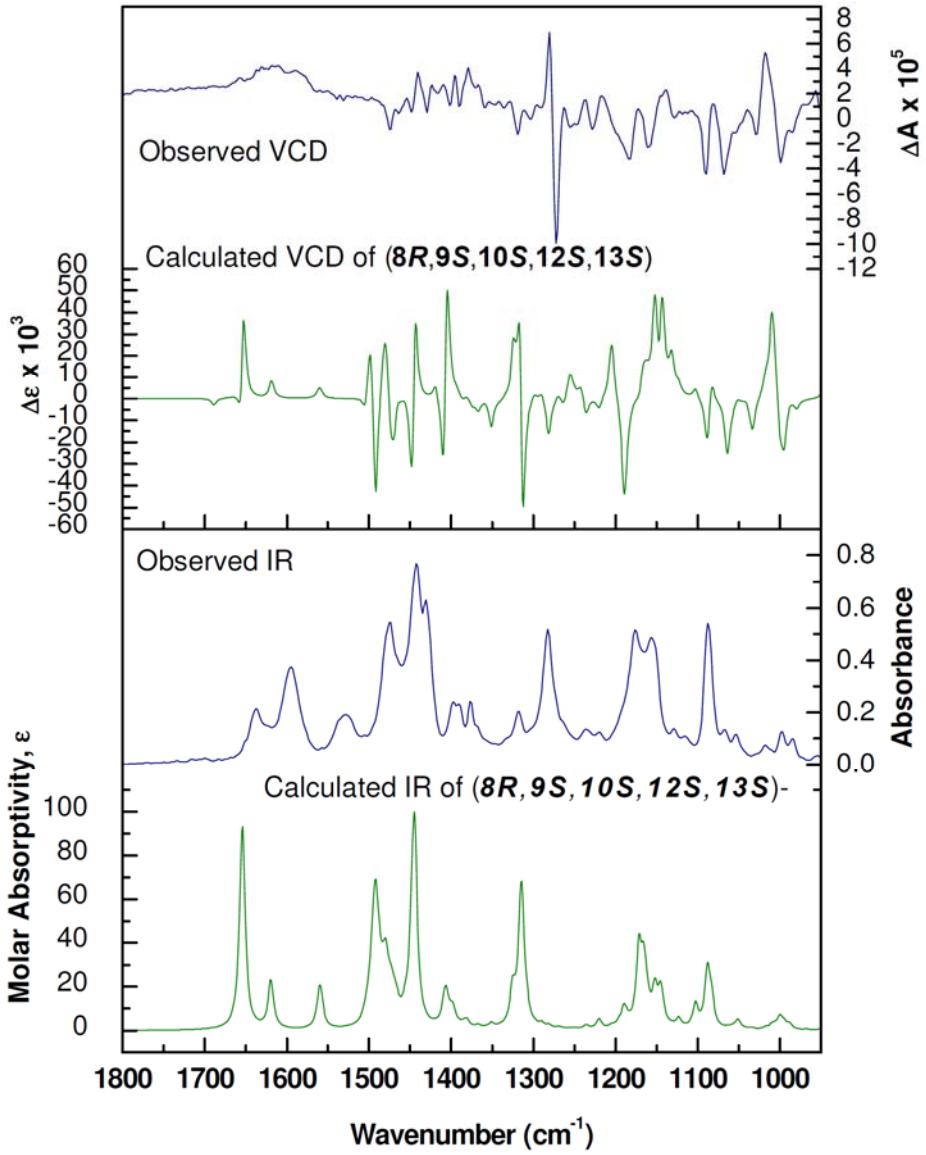

Figure S9. IR (lower frame) and VCD (upper frame) spectra observed for eupenifeldin (right axes) compared with calculated Boltzmann-averaged spectra of the calculated conformations for the 8*R*,9*S*,10*S*,12*S*,13*S* configuration, (left axes).

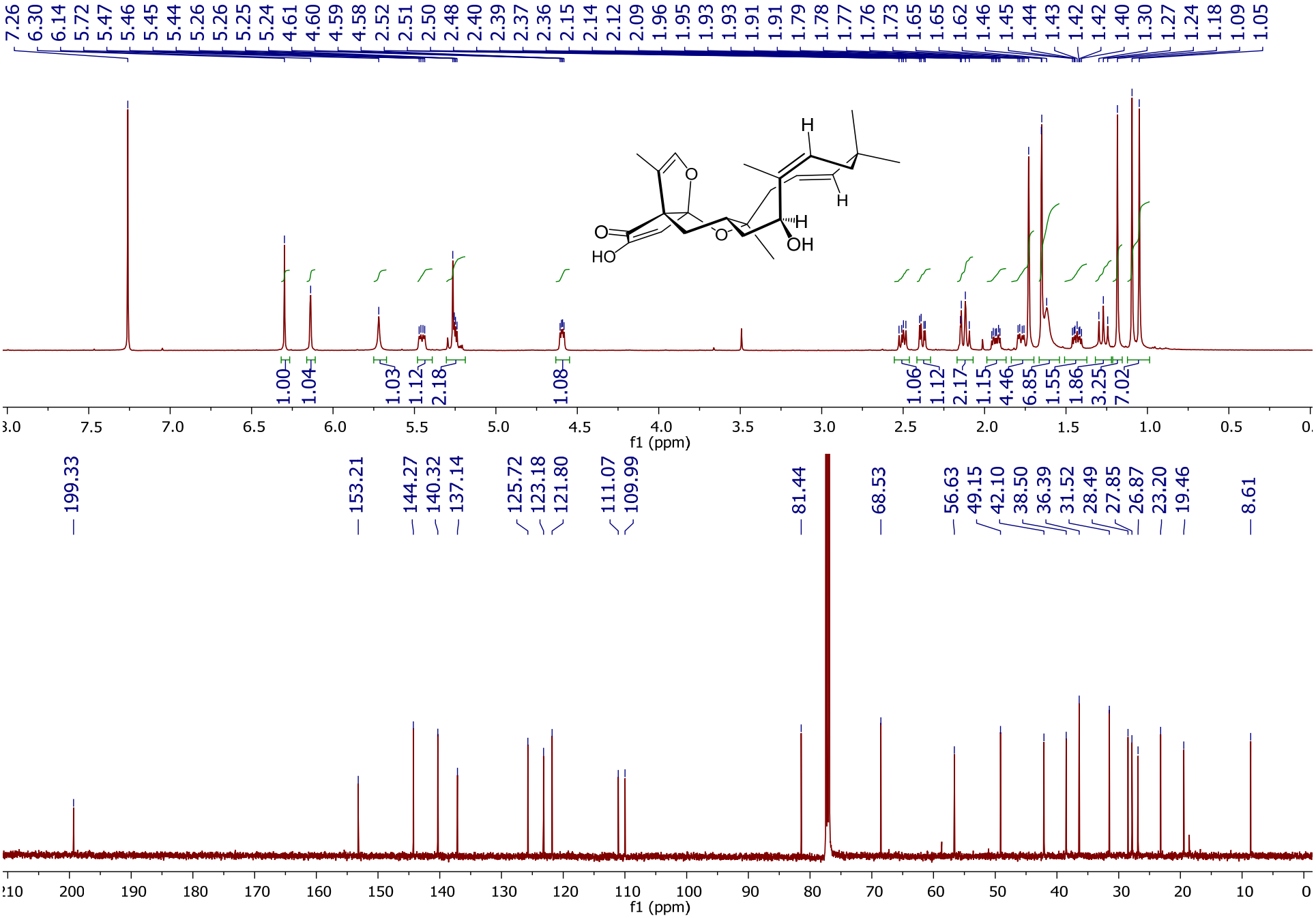

Figure S10. ^{1}H and ^{13}C NMR spectra of compd **1** [500 MHz for ^{1}H and 125 MHz for ^{13}C, $CDCl_3$].

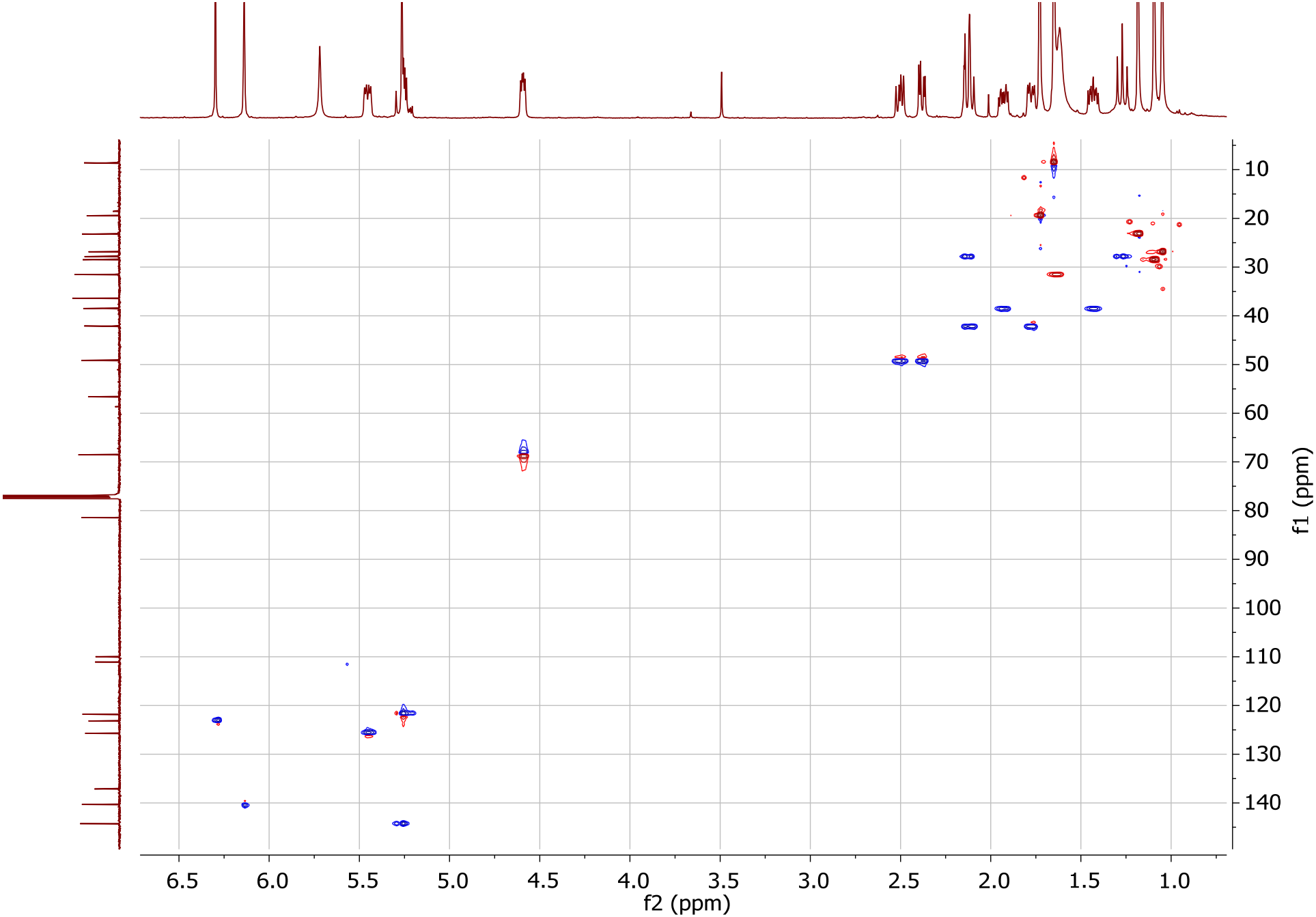

Figure S11. Edited-HSQC NMR spectrum of compd **1** [500 MHz, $CDCl_3$].

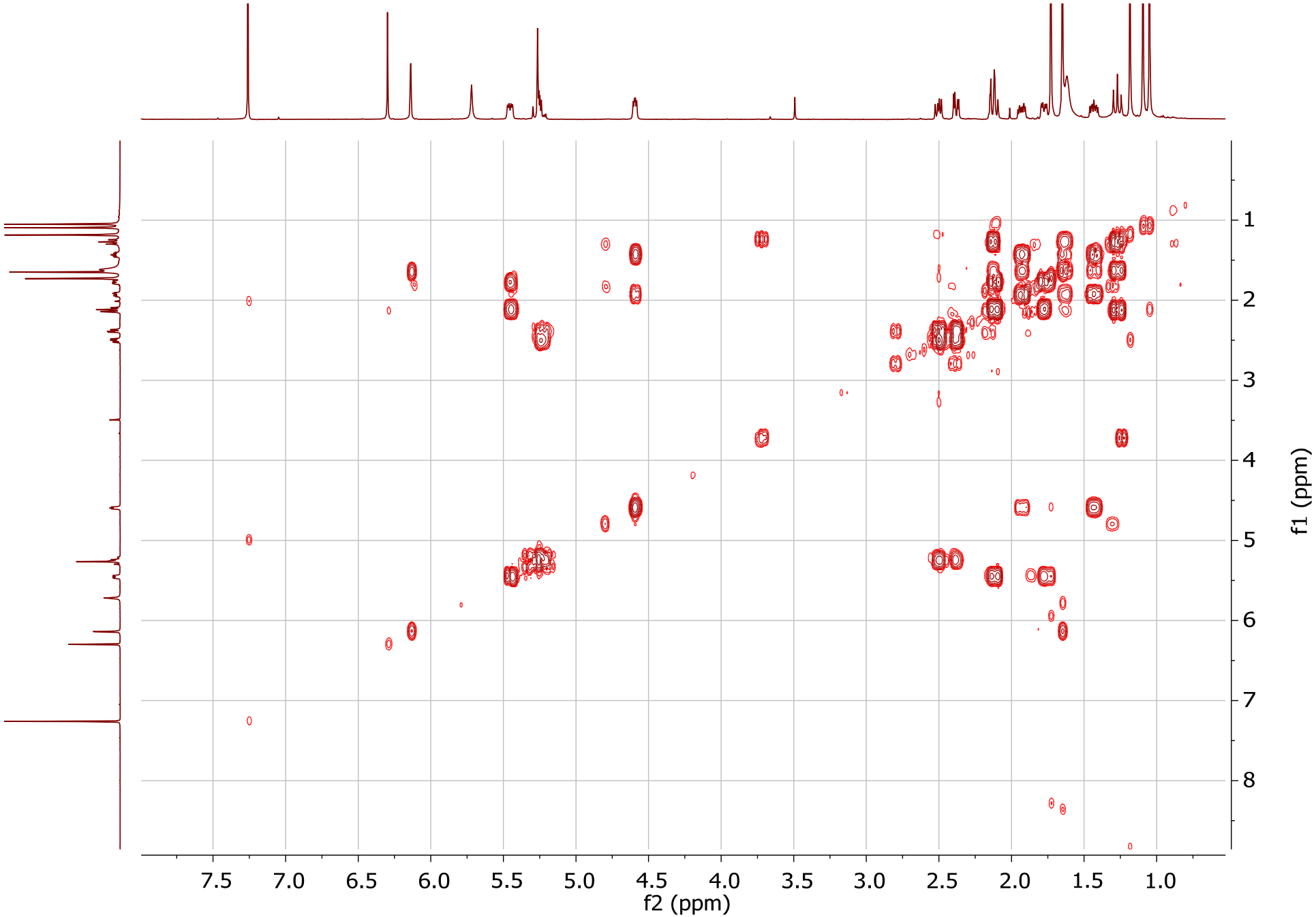

Figure S12. COSY NMR spectrum of compd **1** [500 MHz, $CDCl_3$].

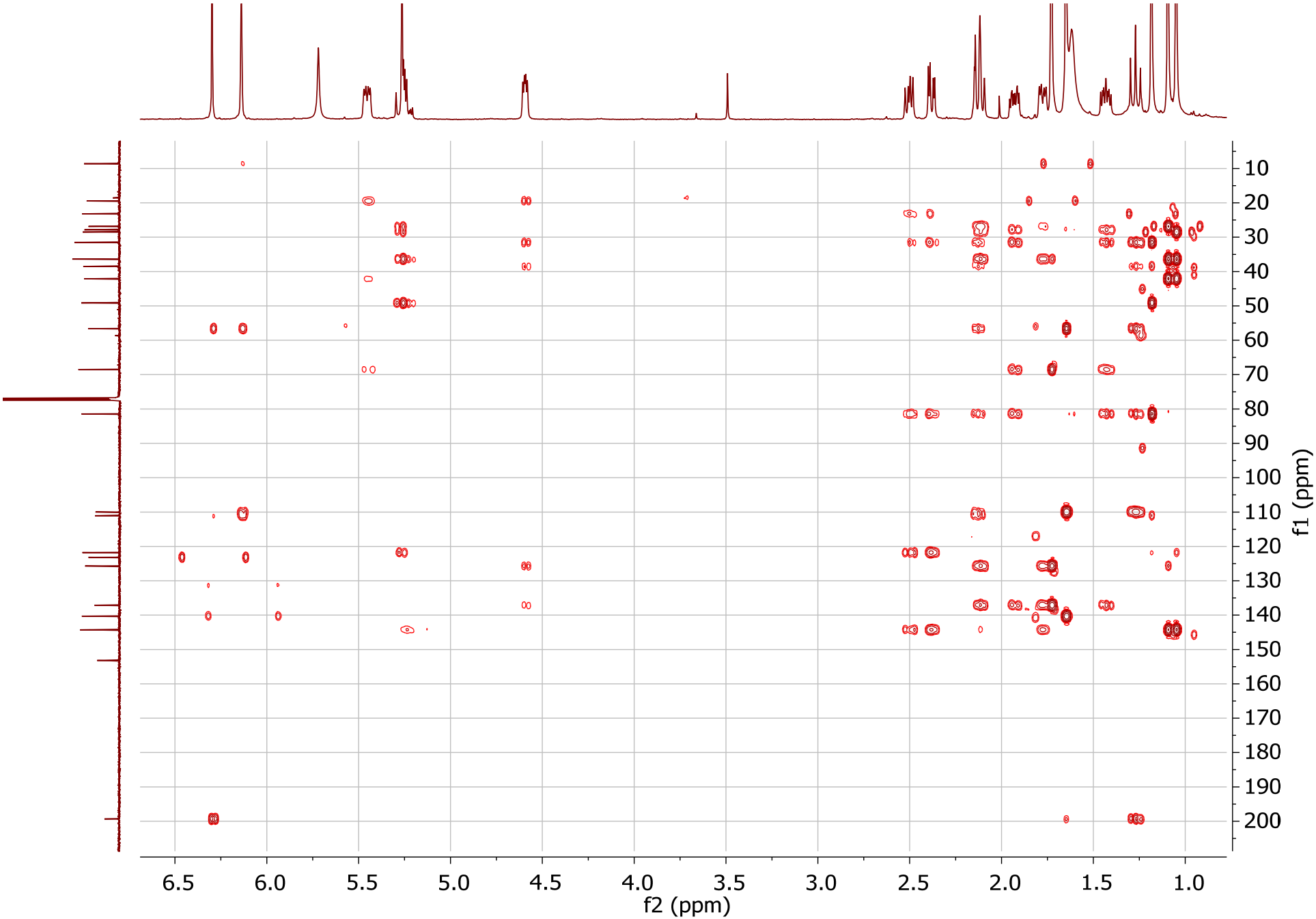

Figure S13. HMBC NMR spectrum of compd **1** [500 MHz, $CDCl_3$].

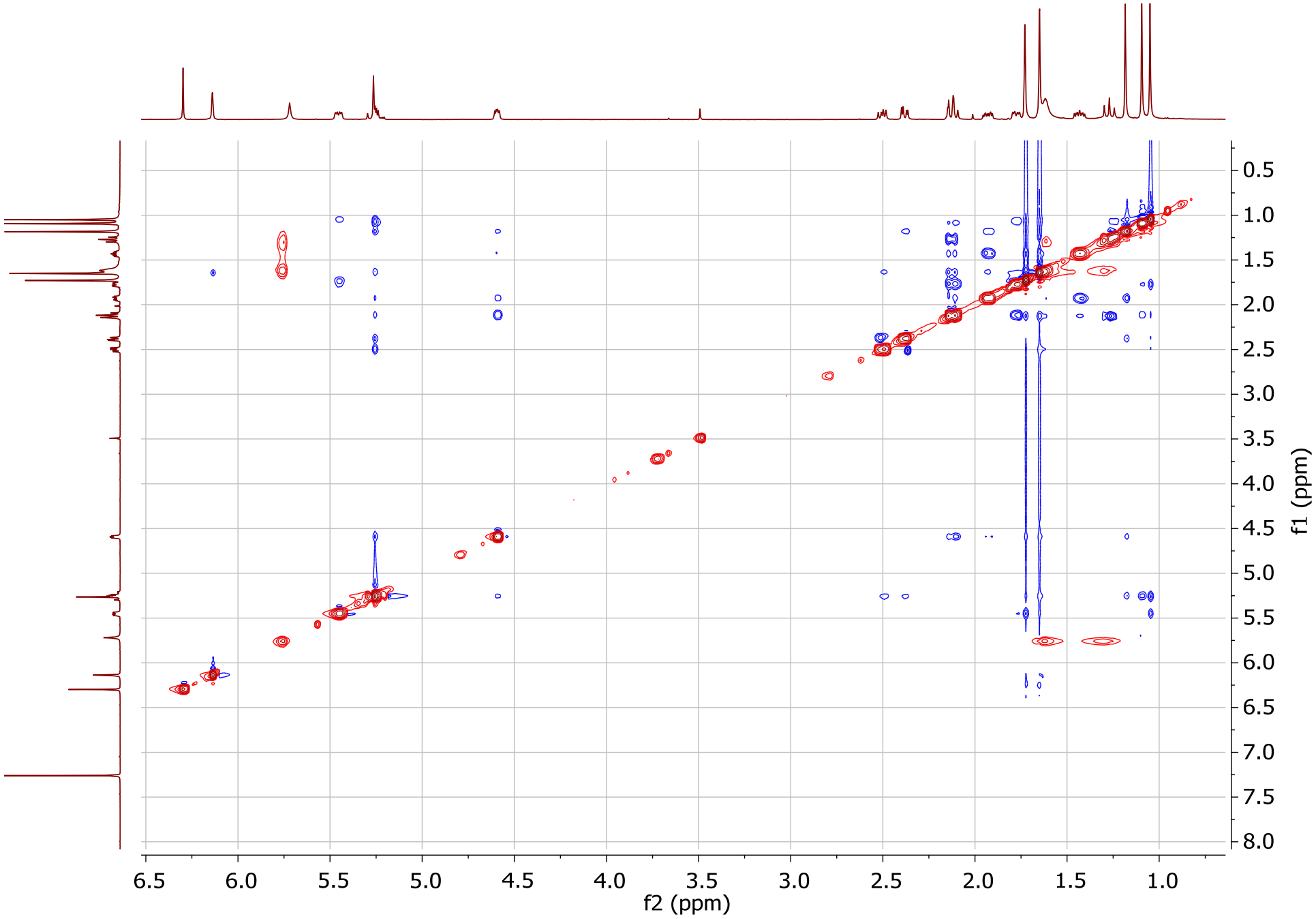

Figure S14. NOESY NMR spectrum of compd **1** [500 MHz, $CDCl_3$].

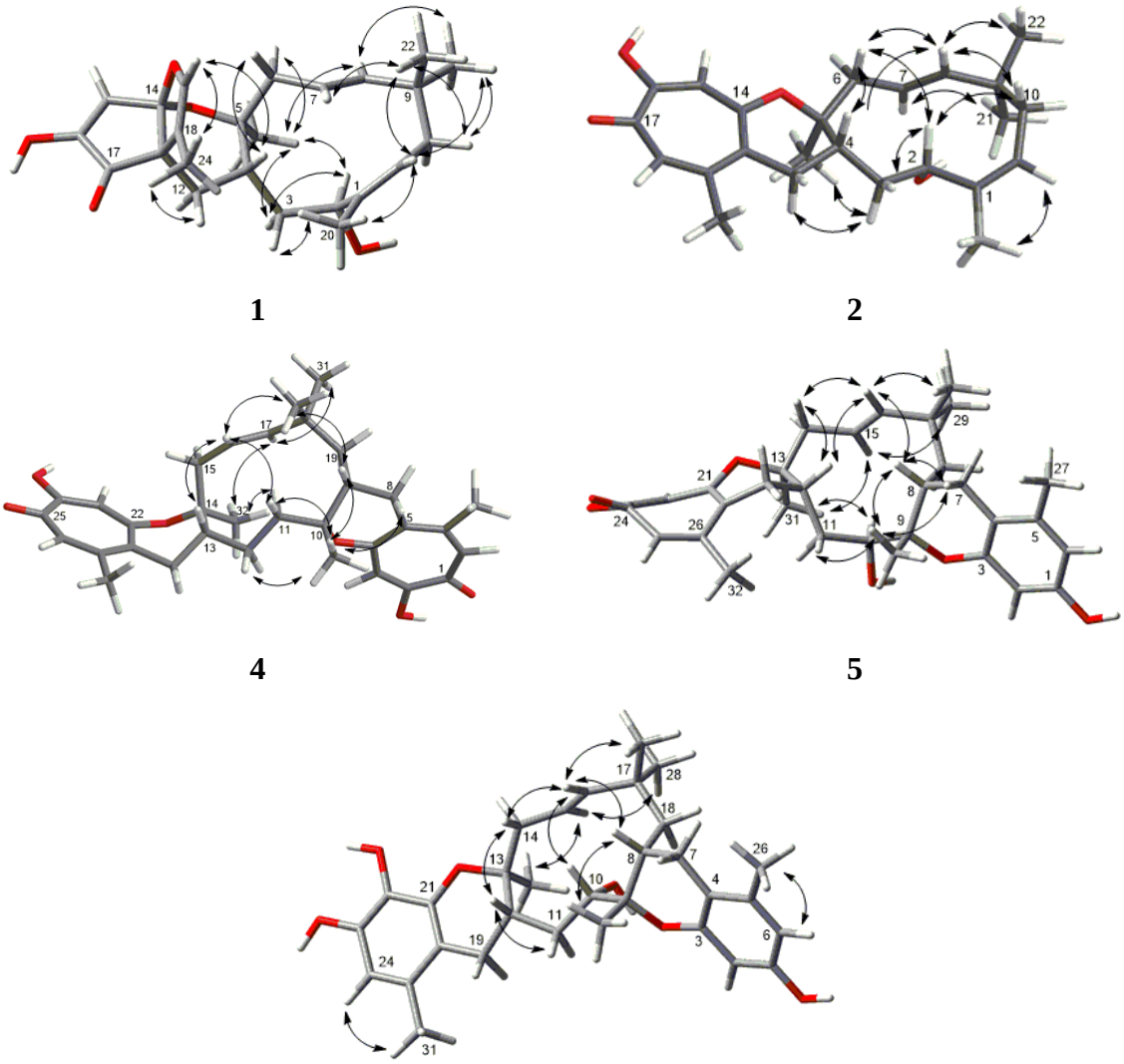

1 **2**

4 **5**

6

Figure S15. Key NOESY correlations of **1**, **2** and **4-6**.

Table S2. ^{13}C NMR data (125 MHz) for **1** in $CDCl_3$, comparing the experimental values vs those predicted by ACD software [ACD/C+H NMR Predictor and DB 2015.2.5, Advanced Chemistry Development, Inc. (Toronto, Canada)].

position	δ_C, experimental	δ_C, predicted	confidence limits
1	137.1	140.0	±2.7
2	68.5	72.2	±5.2
3	38.5	32.8	±5.2
4	31.5	41.8	±1.4
5	81.4	79.5	±4.7
6	49.1	43.6	±5.3
7	121.8	120.8	±1.0
8	144.2	143.4	±1.0
9	36.3	37.0	±0.6
10	42.1	38.9	±1.3
11	125.7	123.7	±3.4
12	27.8	34.1	±2.4
13	56.6	61.5	±5.0
14	111.0	110.8	±4.2
15	123.1	121.6	±16.8
16	153.2	152.3	±5.0
17	199.3	196.3	±2.8
18	109.9	112.8	±16.3
19	140.3	142.9	±5.2
20	19.4	18.5	±2.3
21	28.4	27.2	±0.4
22	26.8	27.2	±0.4
23	23.2	20.0	±2.1
24	8.6	12.0	±4.4

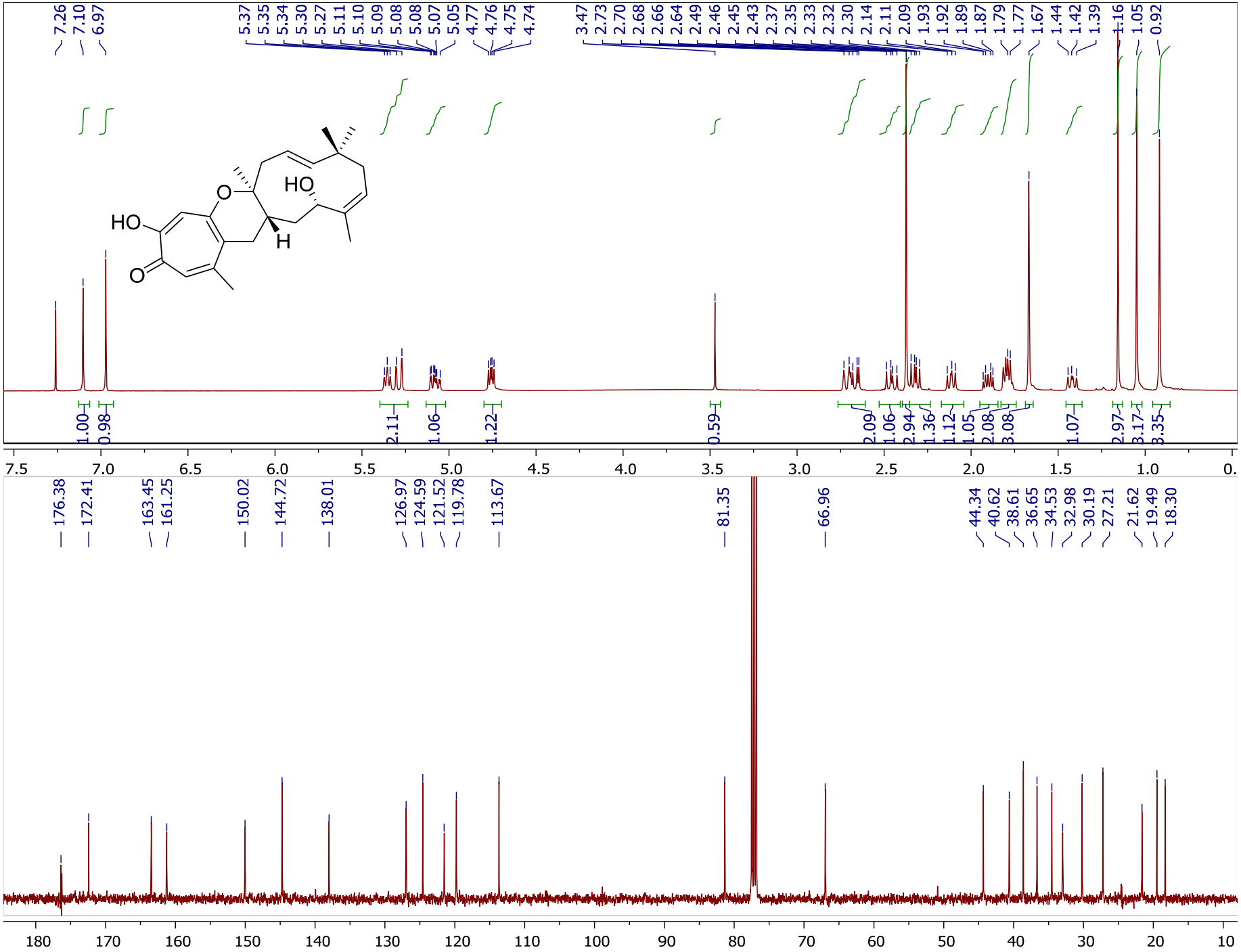

Figure S16. ^{1}H and ^{13}C NMR spectra of compd **2** [500 MHz for ^{1}H and 100 MHz for ^{13}C, $CDCl_3$].

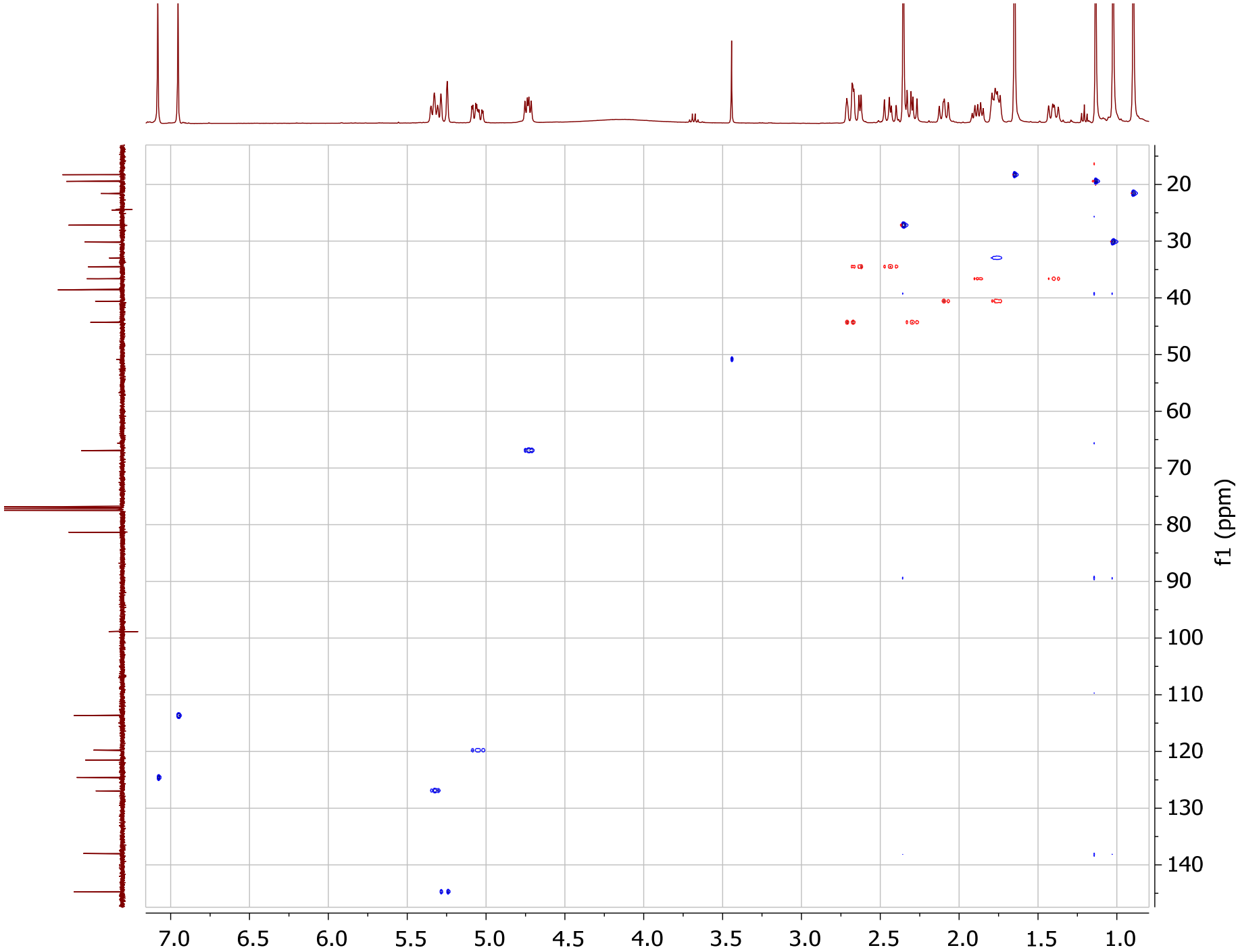

Figure S17. Edited-HSQC NMR spectrum of compd **2** [400 MHz, $CDCl_3$].

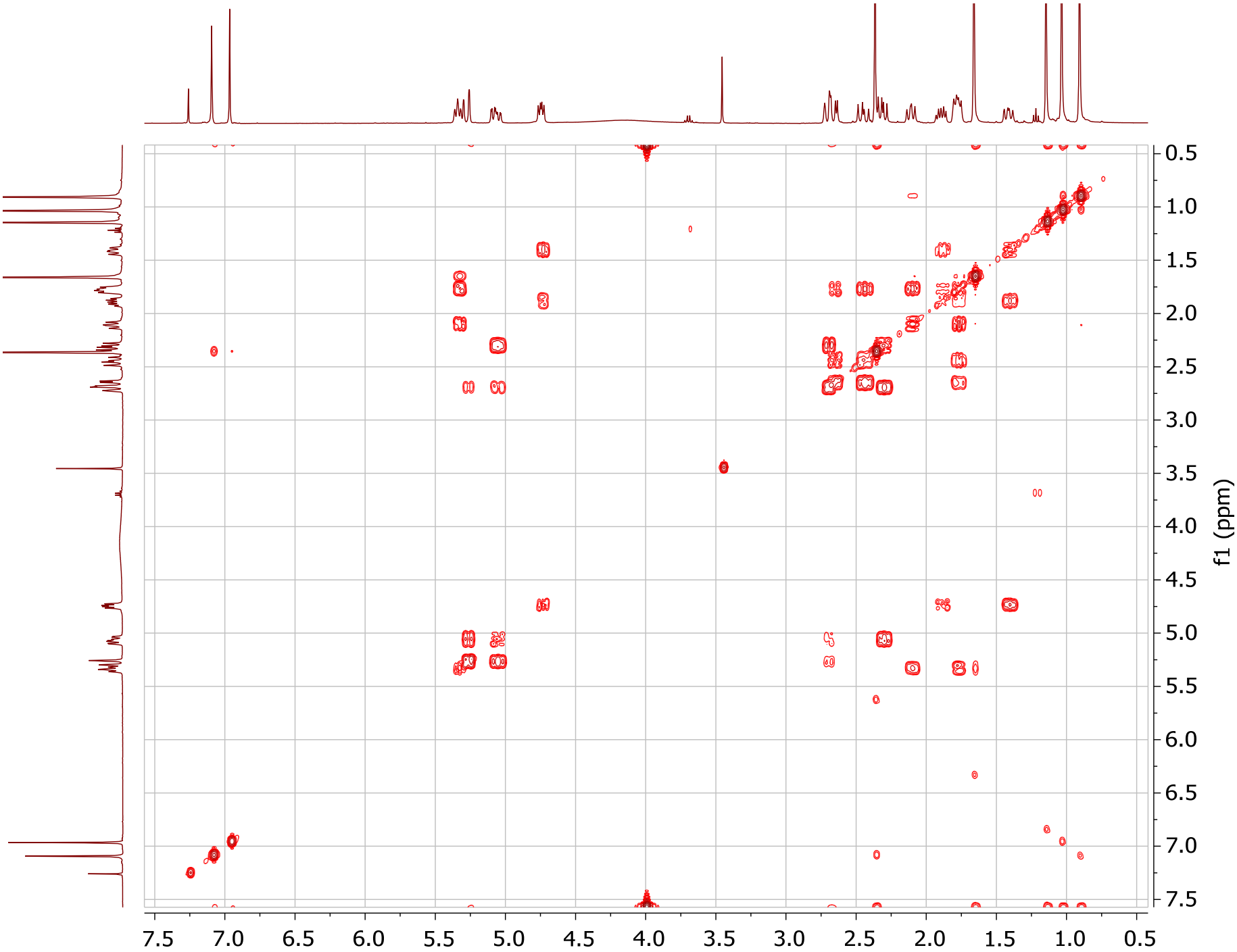

Figure S18. COSY NMR spectrum of compd **2** [400 MHz, $CDCl_3$].

Figure S19. HMBC NMR spectrum of compd **2** [400 MHz, $CDCl_3$].

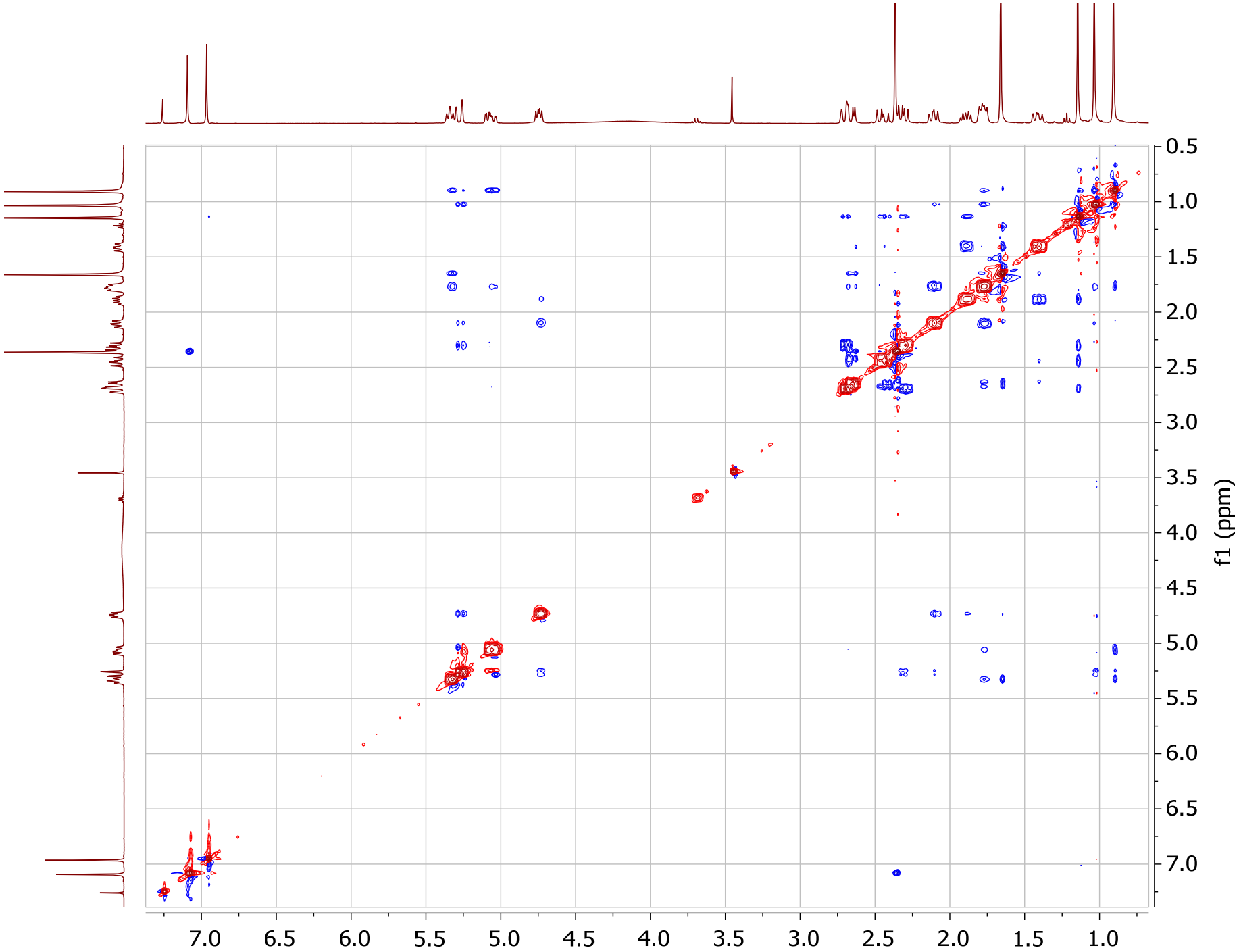

Figure S20. NOESY NMR spectrum of compd **2** [400 MHz, $CDCl_3$].

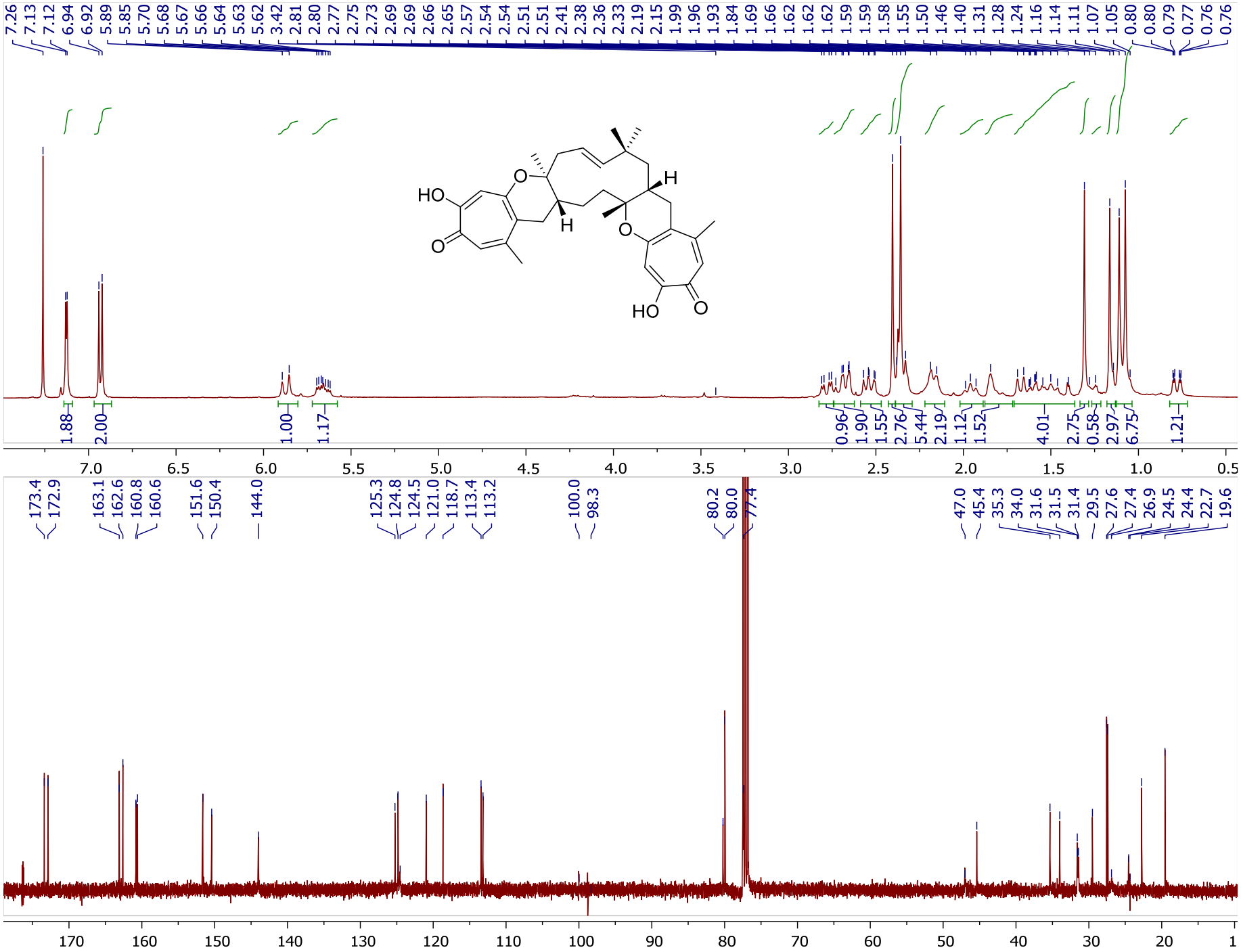

Figure S21. ^{1}H and ^{13}C NMR spectra of compd **4** [400 MHz for ^{1}H and 100 MHz for ^{13}C, $CDCl_3$].

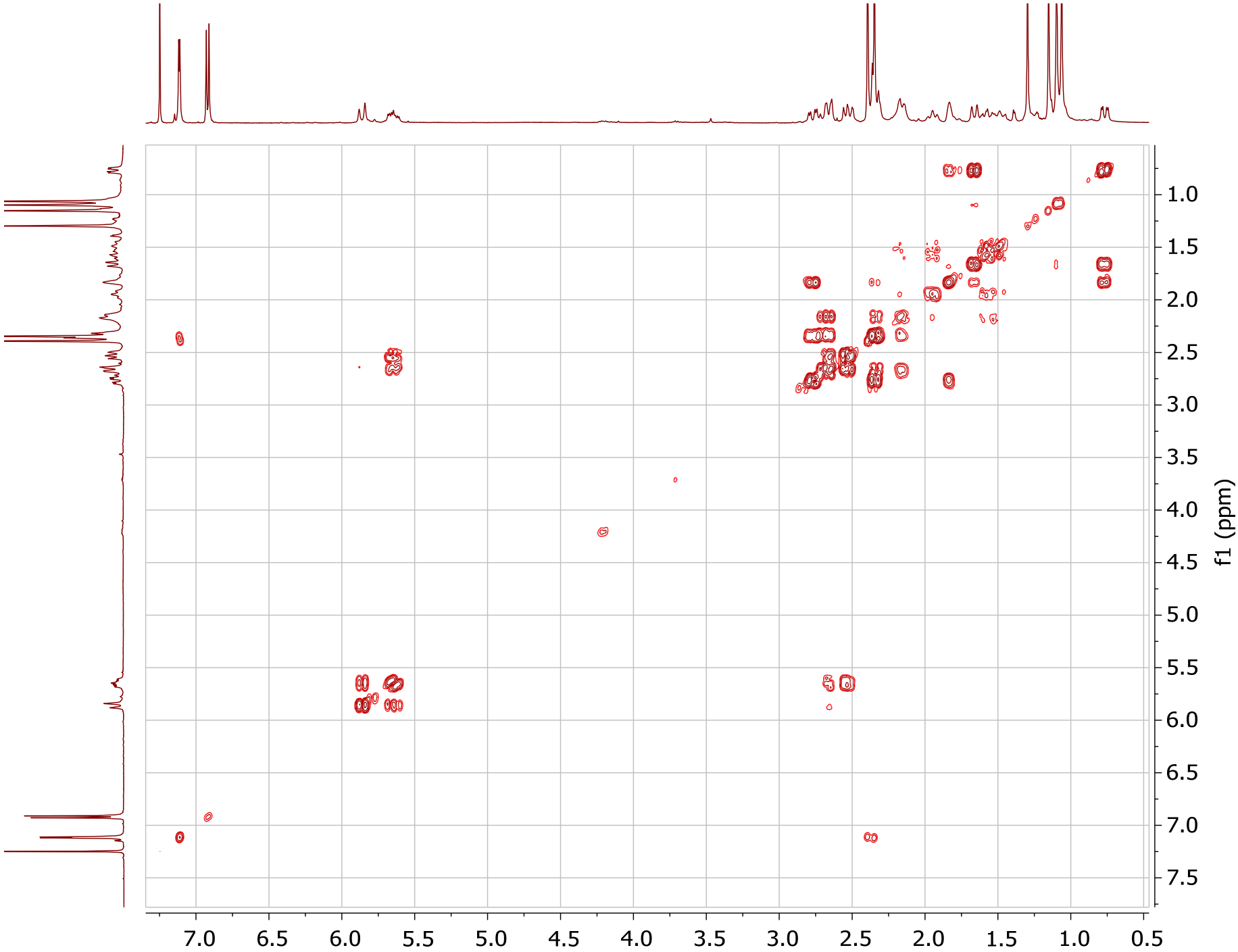

Figure S22. COSY NMR spectra of compd **4** [400 MHz, $CDCl_3$].

Figure S23. Edited-HSQC NMR spectra of compd **4** [400 MHz, $CDCl_3$].

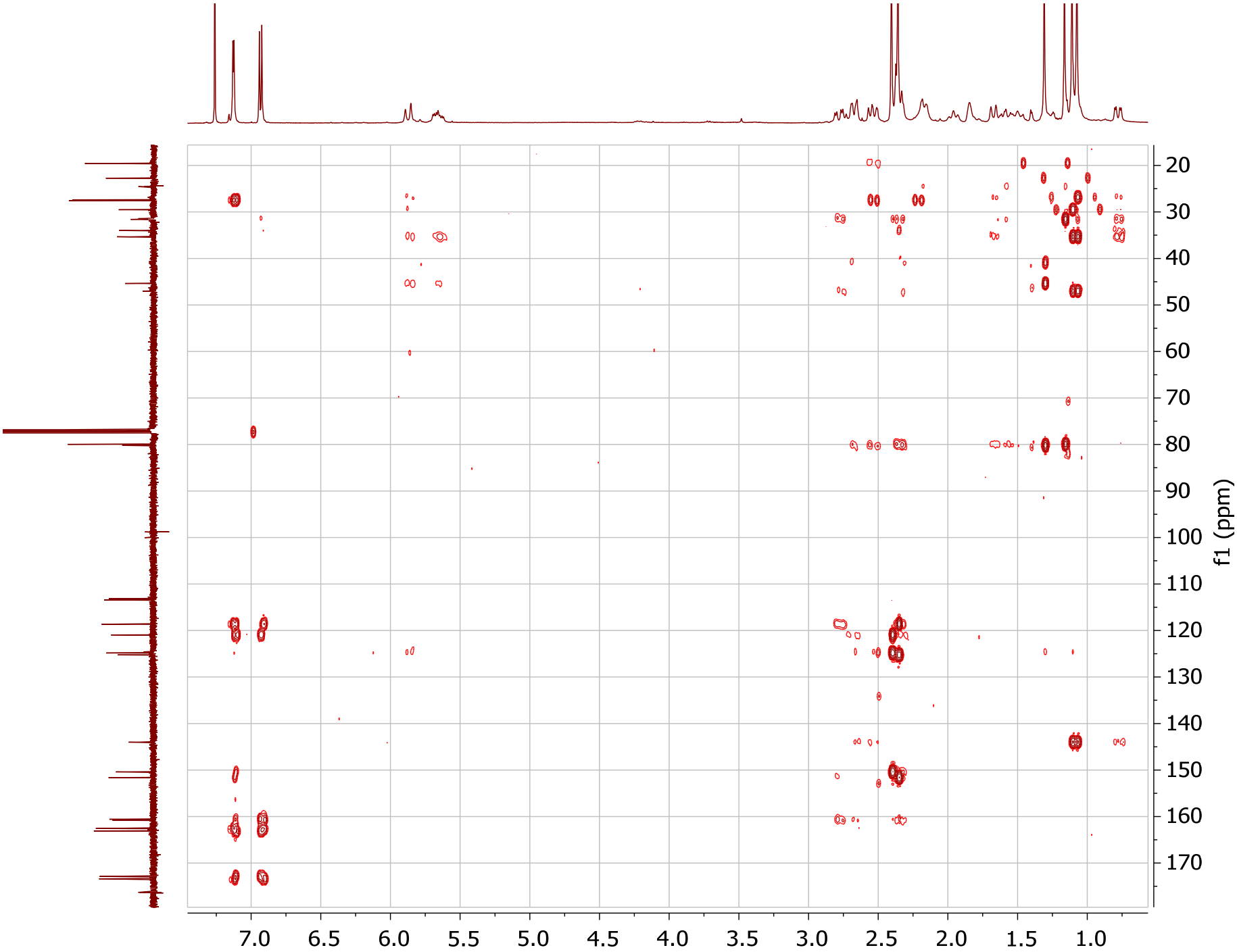

Figure S24. HMBC NMR spectra of compd **4** [400 MHz, $CDCl_3$].

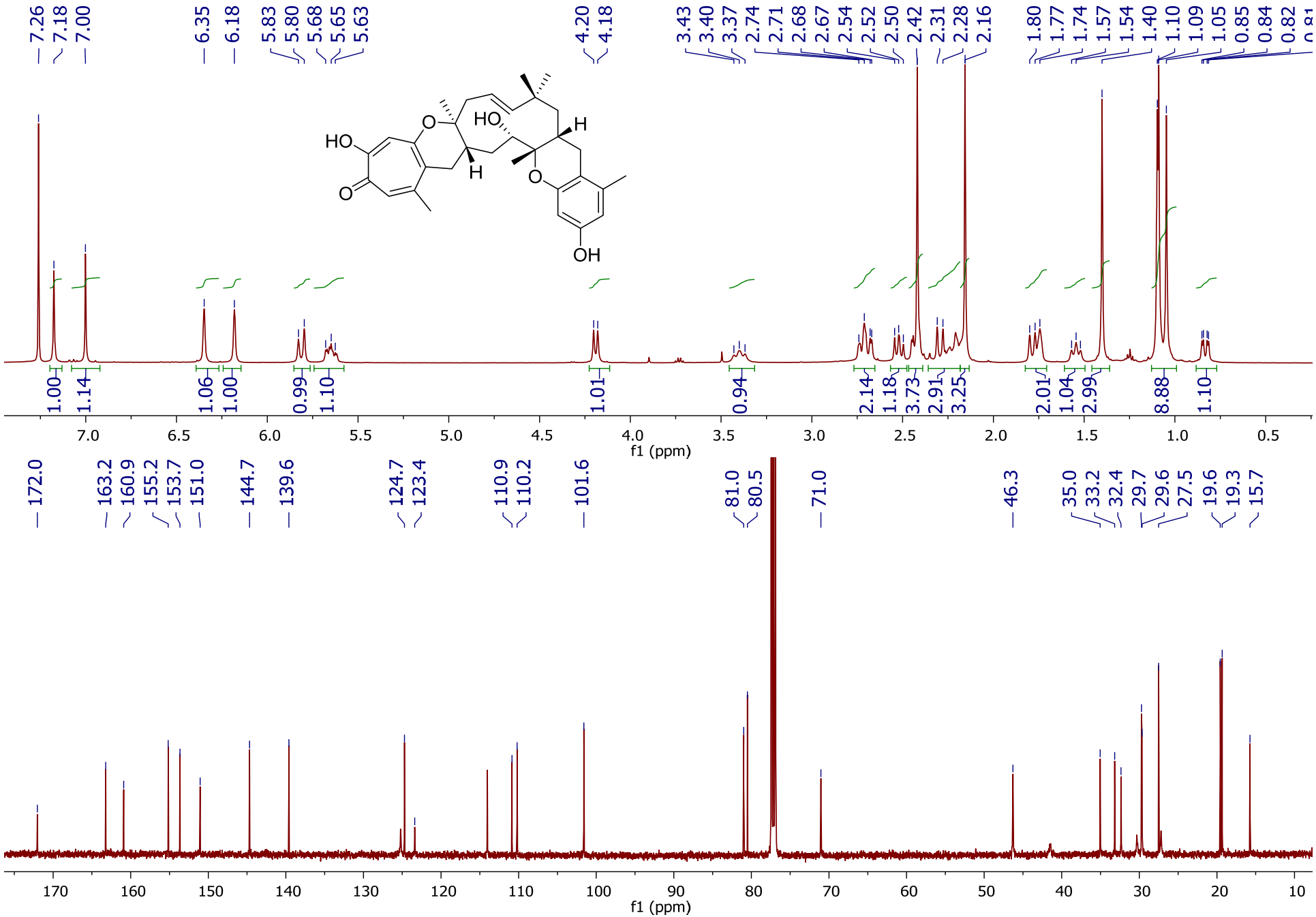

Figure S25. ^{1}H and ^{13}C NMR spectra of compd **5** [500 MHz for ^{1}H and 125 MHz for ^{13}C, $CDCl_3$].

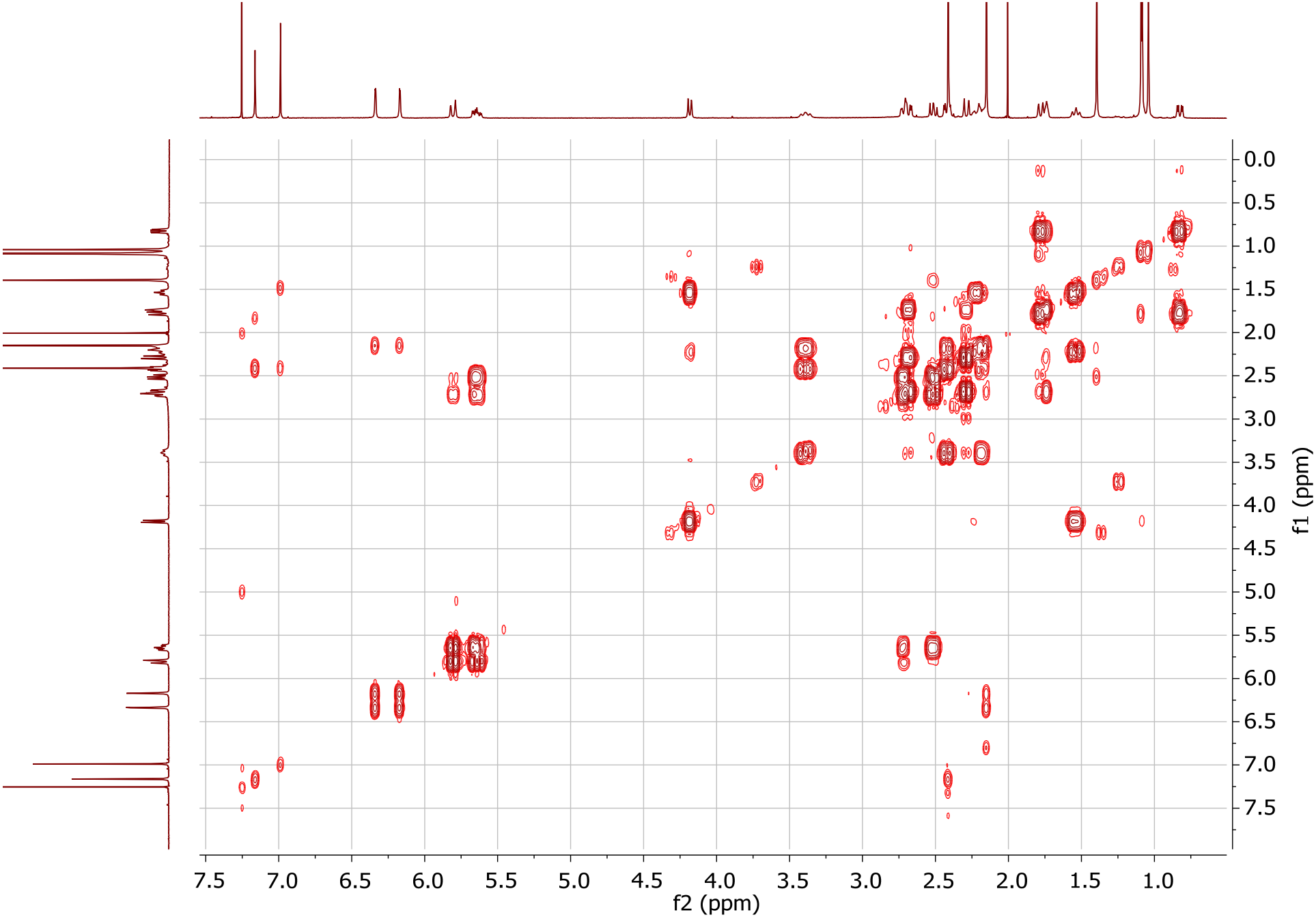

Figure S26. COSY NMR spectrum of compd **5** [500 MHz, $CDCl_3$].

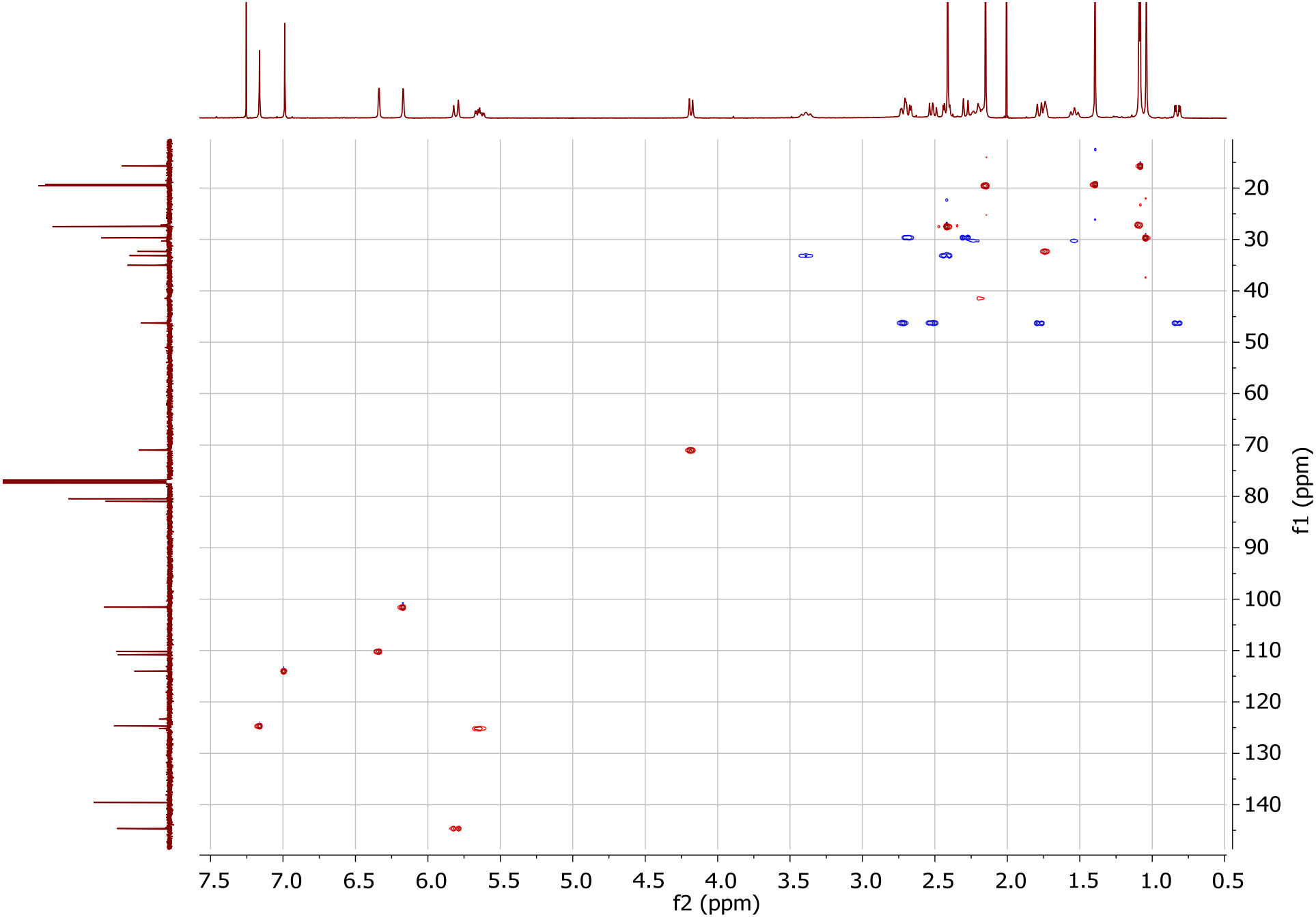

Figure S27. Edited-HSQC NMR spectrum of compd **5** [500 MHz, $CDCl_3$].

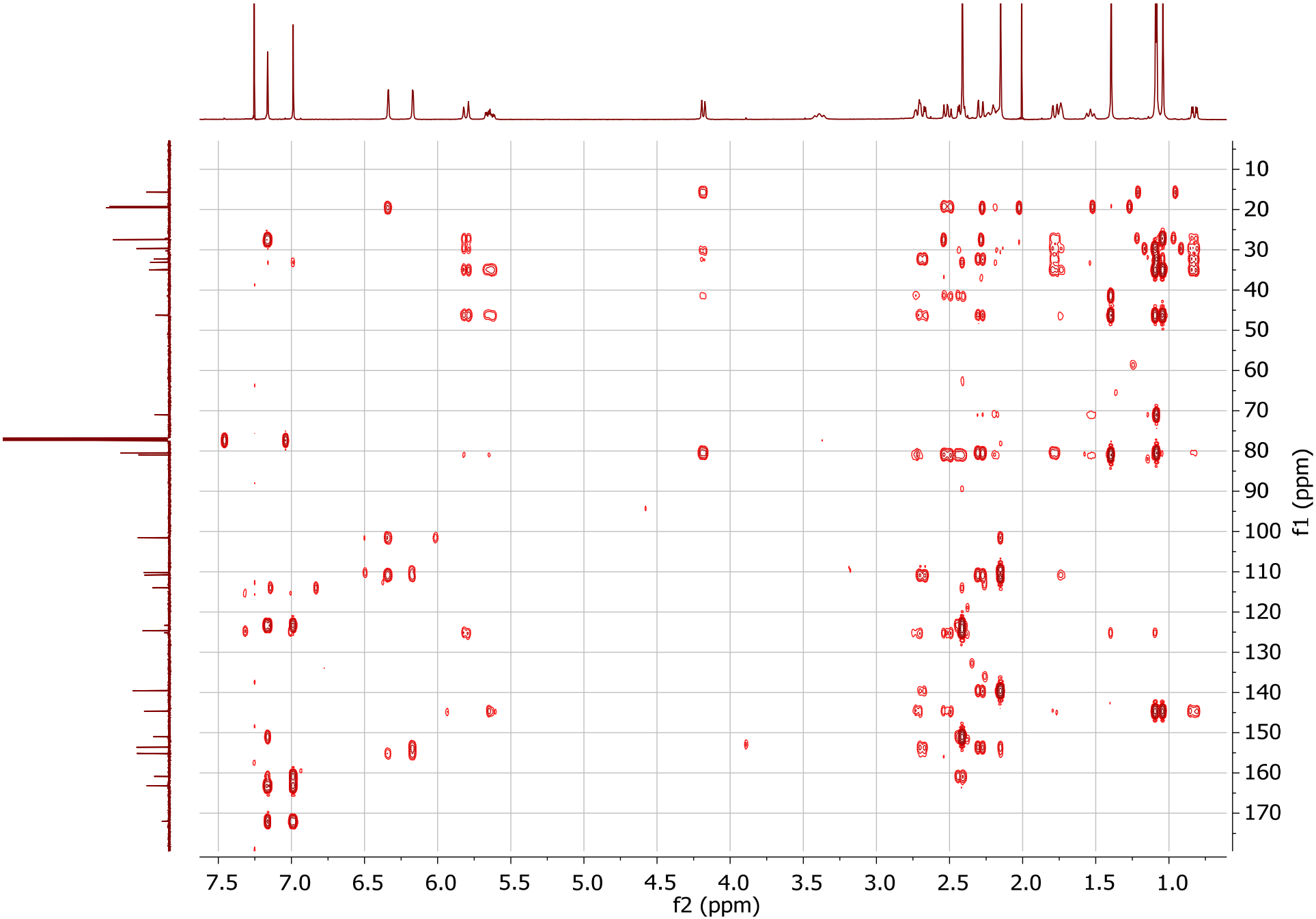

Figure S28. HMBC NMR spectrum of compd **5** [500 MHz, $CDCl_3$].

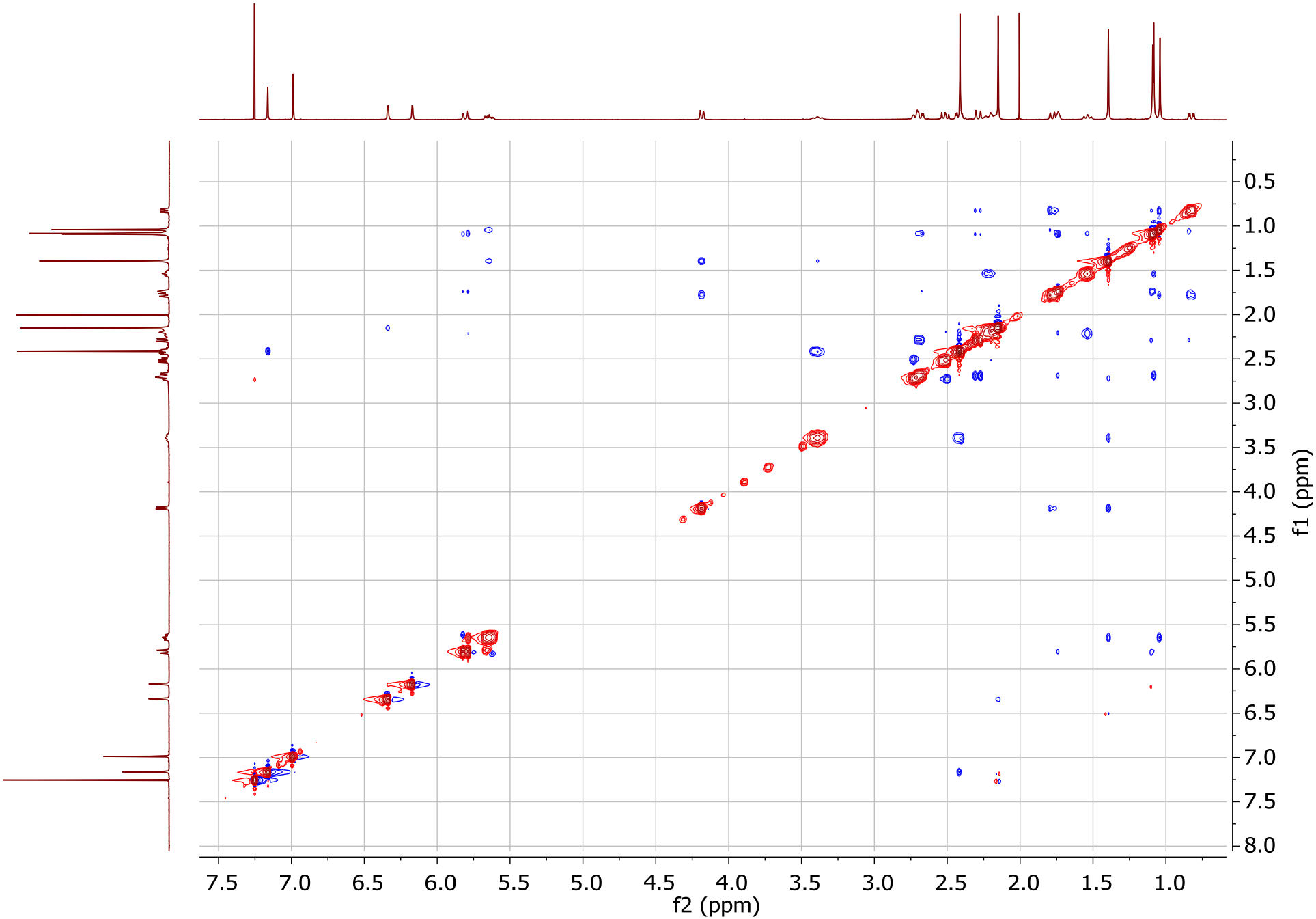

Figure S29. NOESY NMR spectrum of compd **5** [500 MHz, $CDCl_3$].

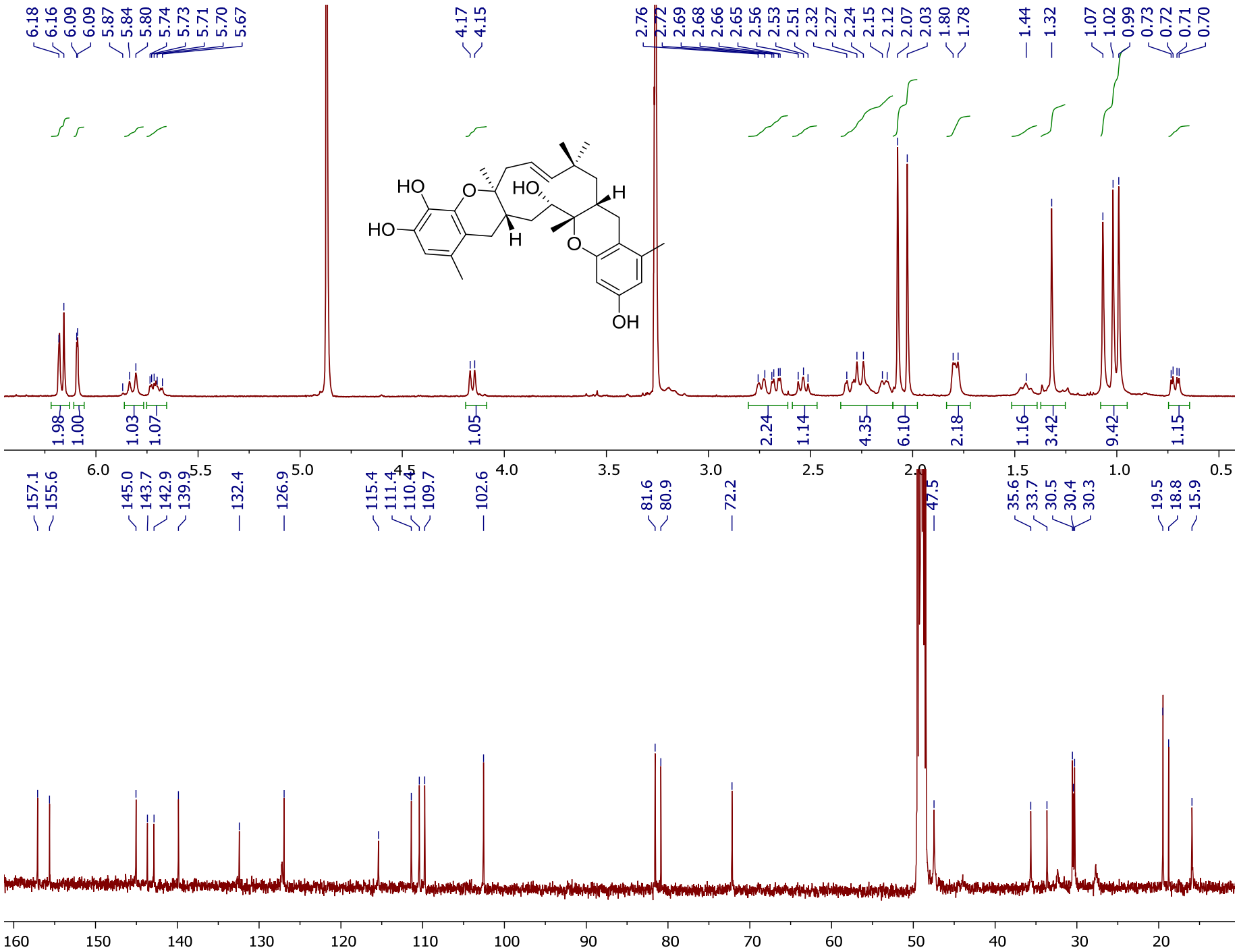

Figure S30. ^{1}H and ^{13}C NMR spectra of compd **6** [500 MHz for ^{1}H and 125 MHz for ^{13}C, Methanol-d_5].

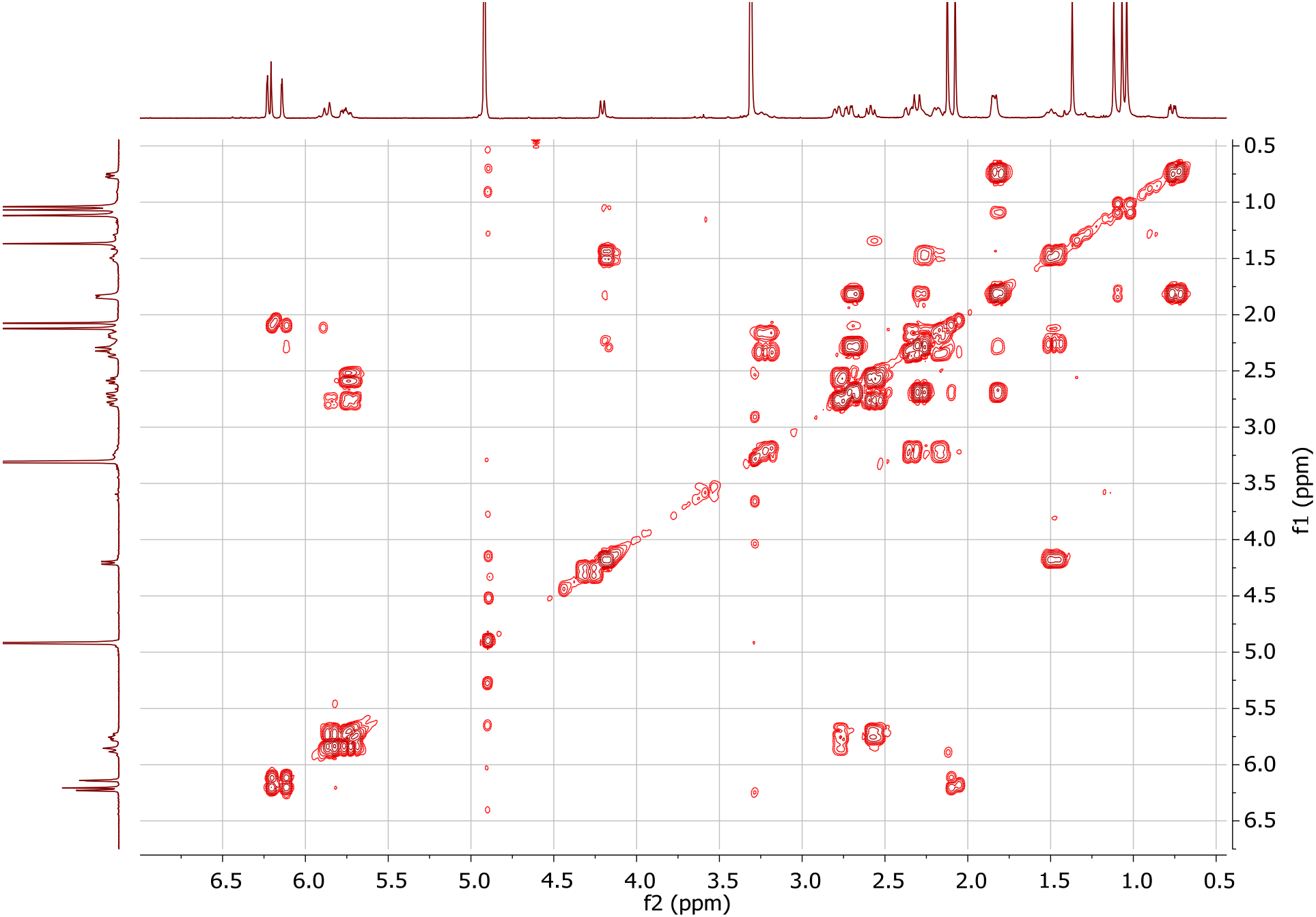

Figure S31. COSY NMR spectrum of compd **6** [400 MHz, Methanol-d_5].

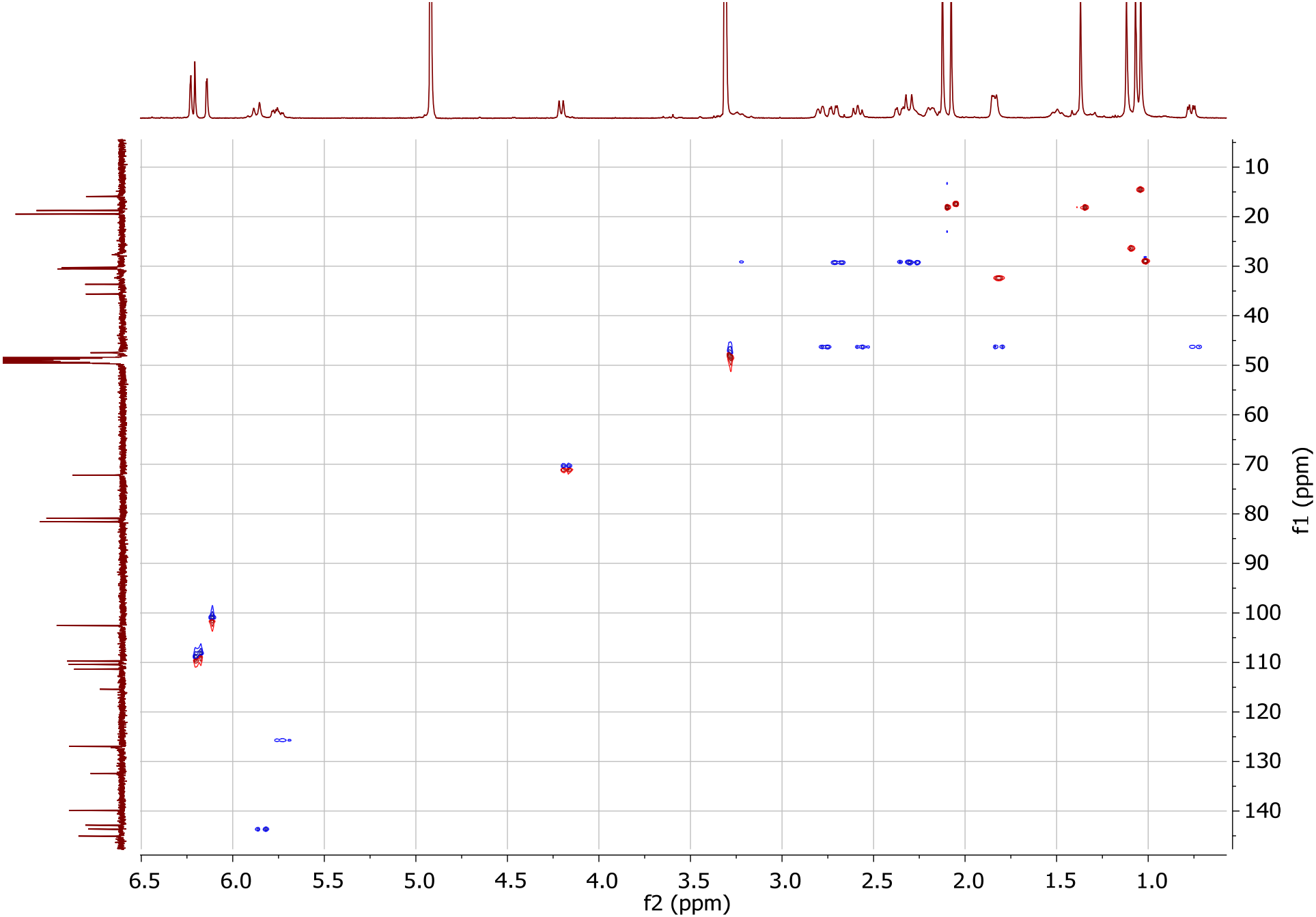

Figure S32. Edited-HSQC NMR spectrum of compd **6** [400 MHz, Methanol-d_5].

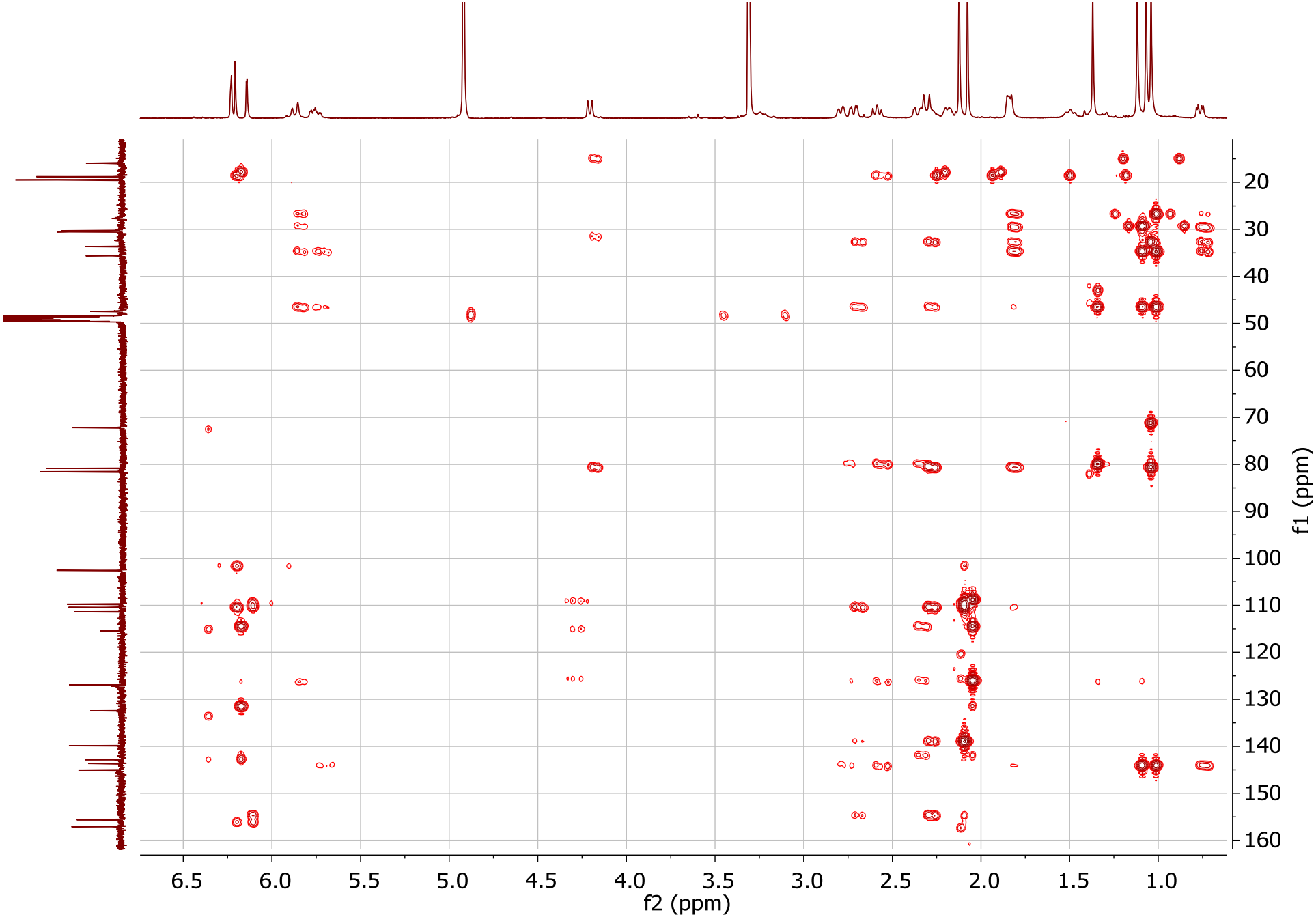

Figure S33. HMBC NMR spectrum of compd **6** [400 MHz, Methanol-d_5].

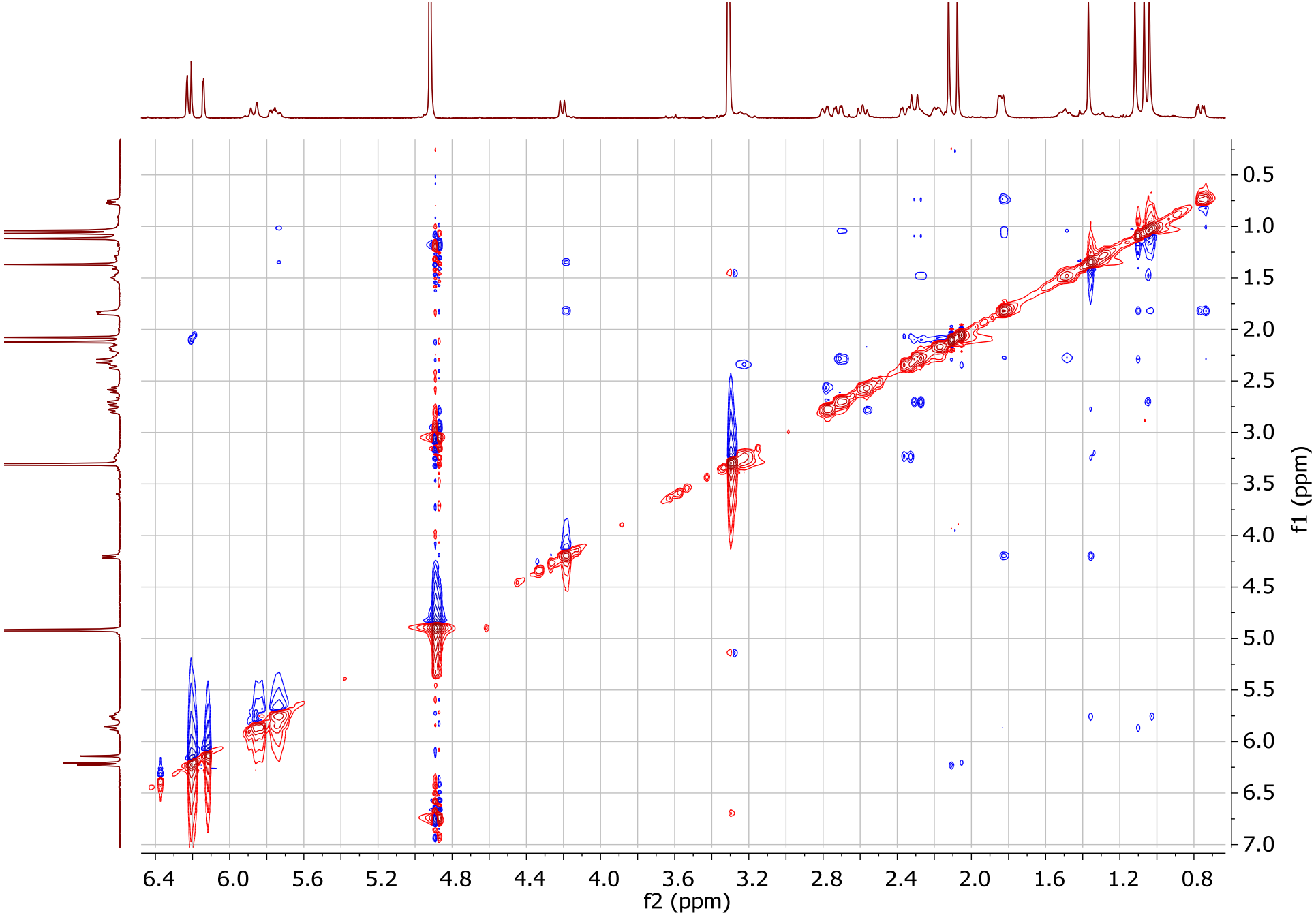

Figure S34. NOESY NMR spectrum of compd **6** [500 MHz, Methanol-d_5].

Compd **1**

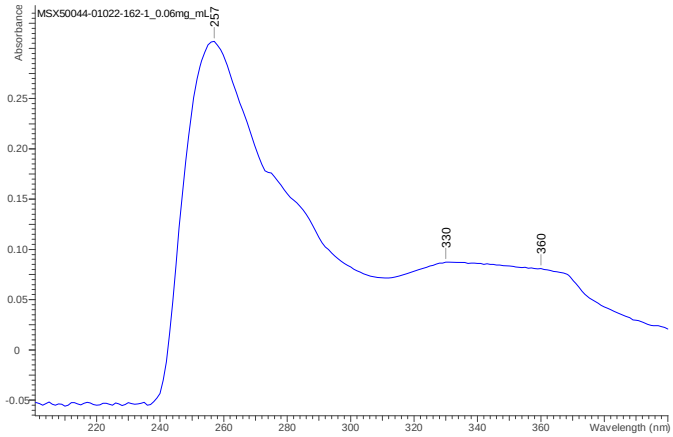

Compd **2**

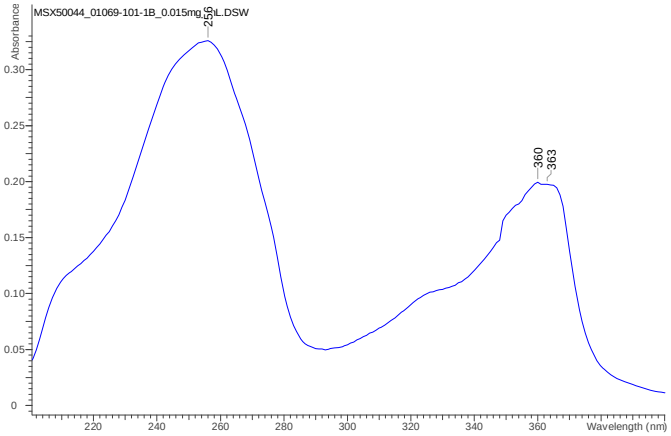

Compd **4**

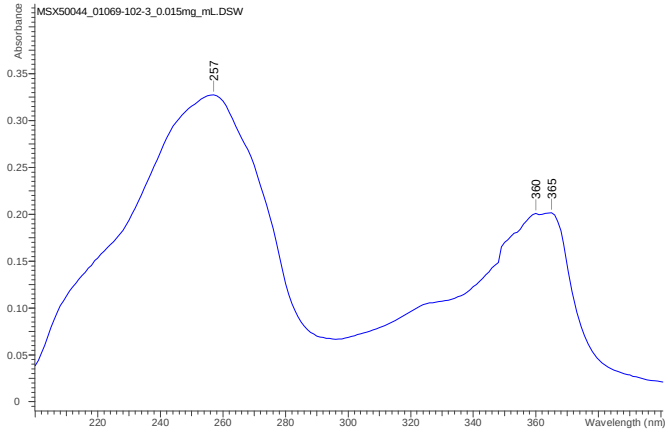

Compd **5**

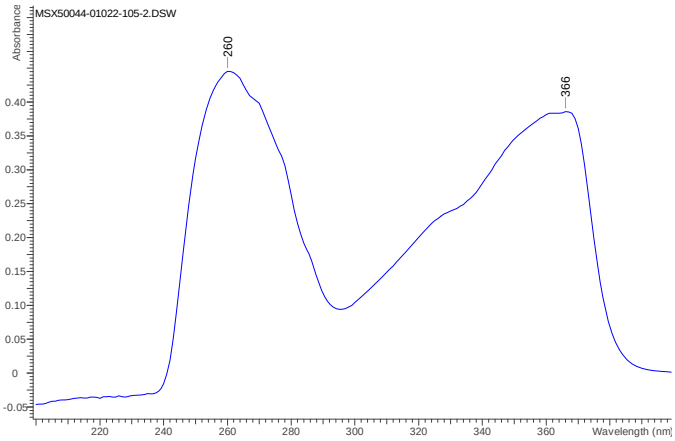

Compd **6**

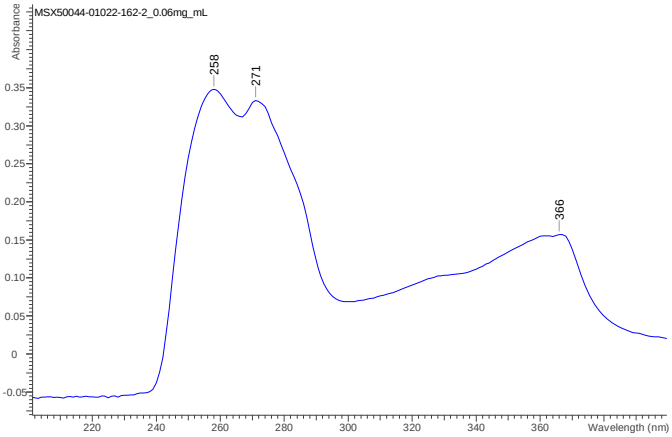

Figure S35. UV spectra of compounds **1, 2, 4-6** analyzed in MeOH.

Compd **1**

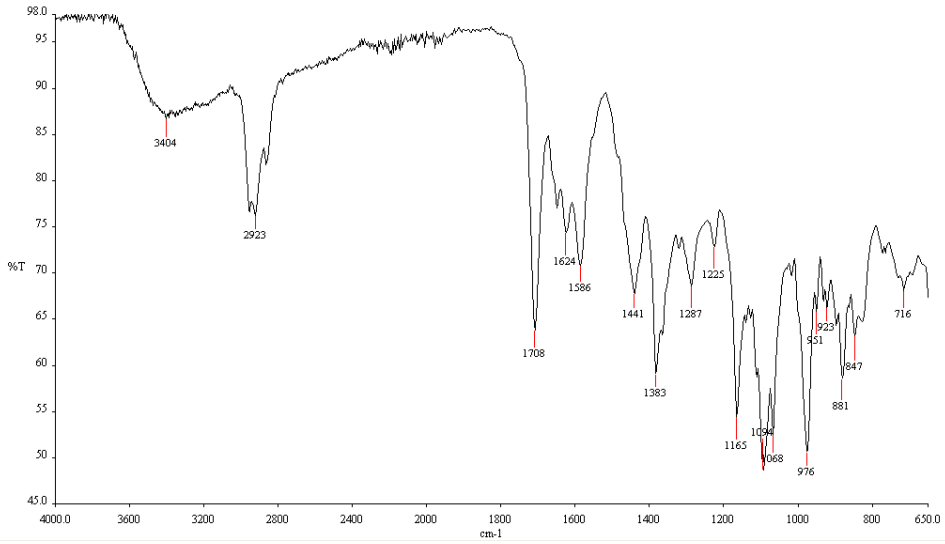

Compd **2**

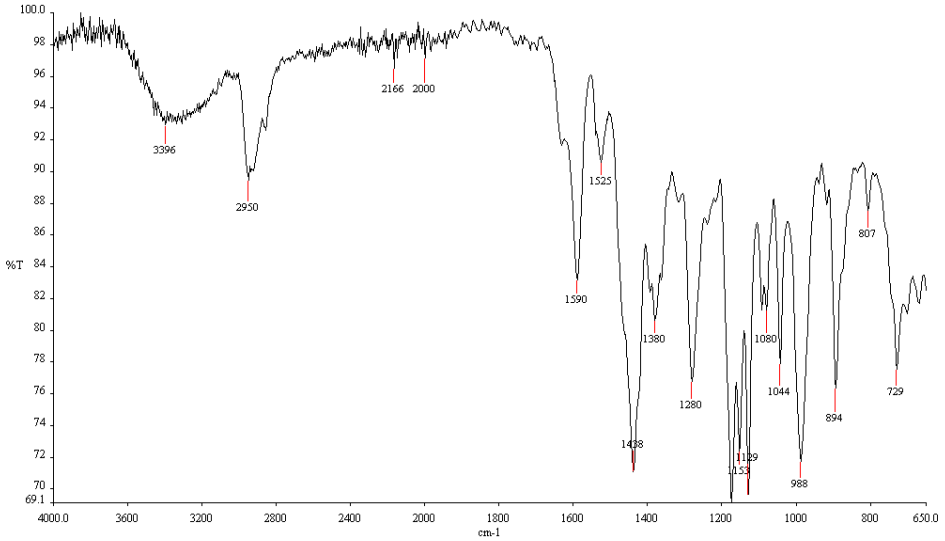

Compd **4**

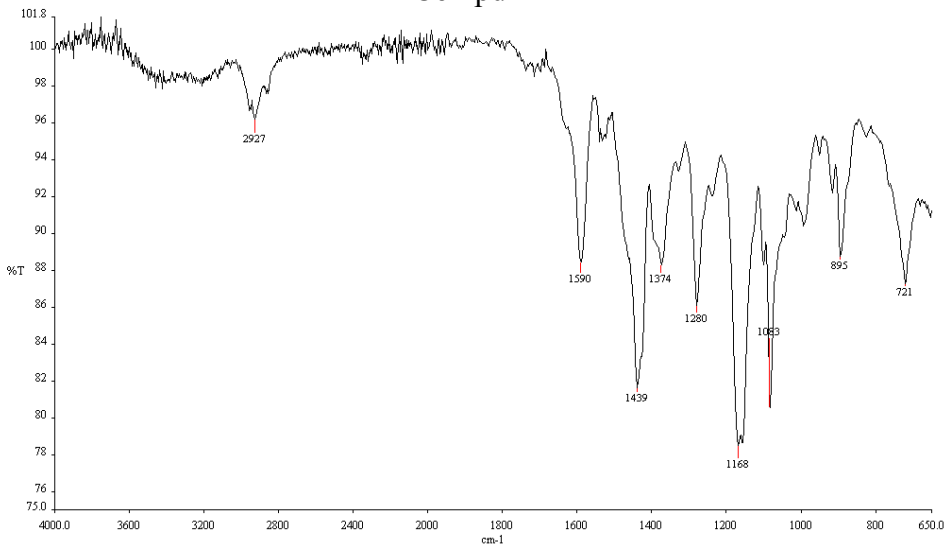

Figure S36. IR spectra of compounds **1, 2, 4-6**.

Compd **5**

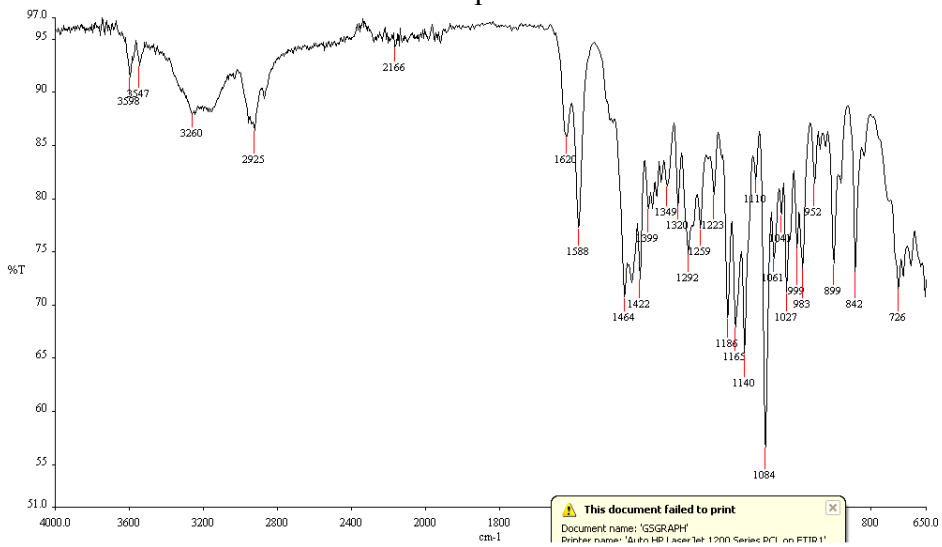

Compd **6**

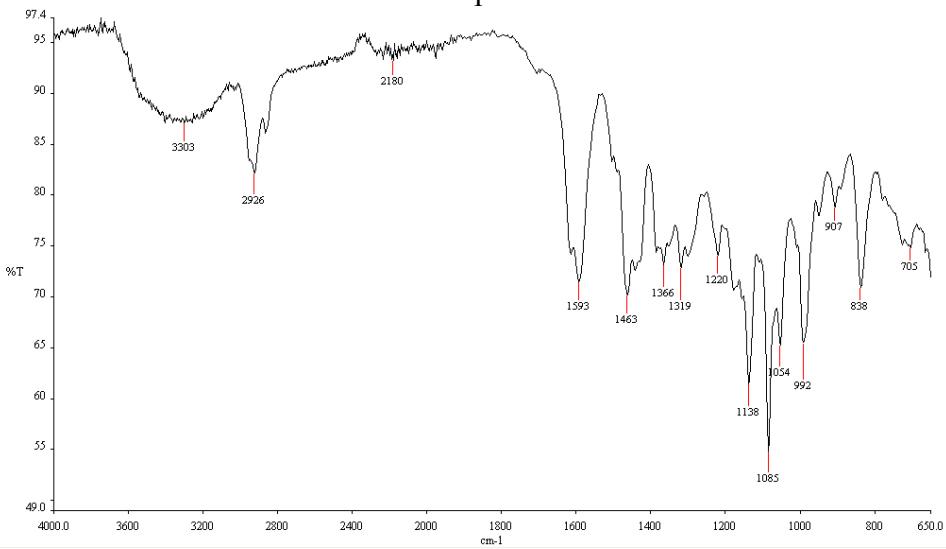

Cont. Figure S36. IR spectra of compounds **1, 2, 4-6**.

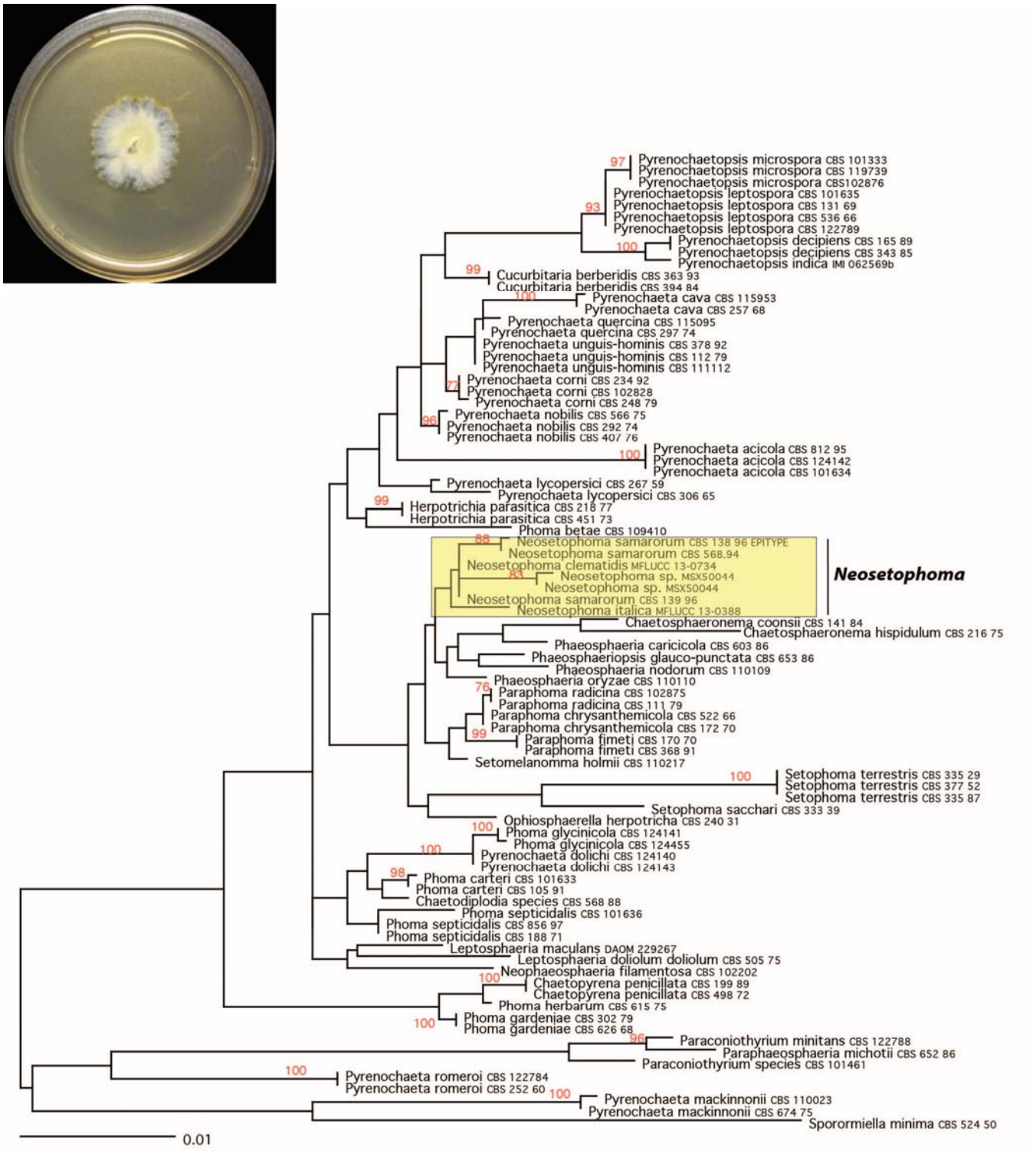

Figure S37. Phylogram of the most likely tree (-lnL = 7011.32) from a PHYML analysis of 84 taxa based on LSU sequence data (2265 bp). Numbers refer to PHYML bootstrap support values ≥ 70% based on 1000 replicates. Strain MSX50044 is identified as *Neosetophoma* sp. (Box highlighted in yellow) as it groups with other *Neosetophoma* spp. described previously. A 3-week old culture on Malt Extract agar media is shown. Bar indicates nucleotide substitutions per site.

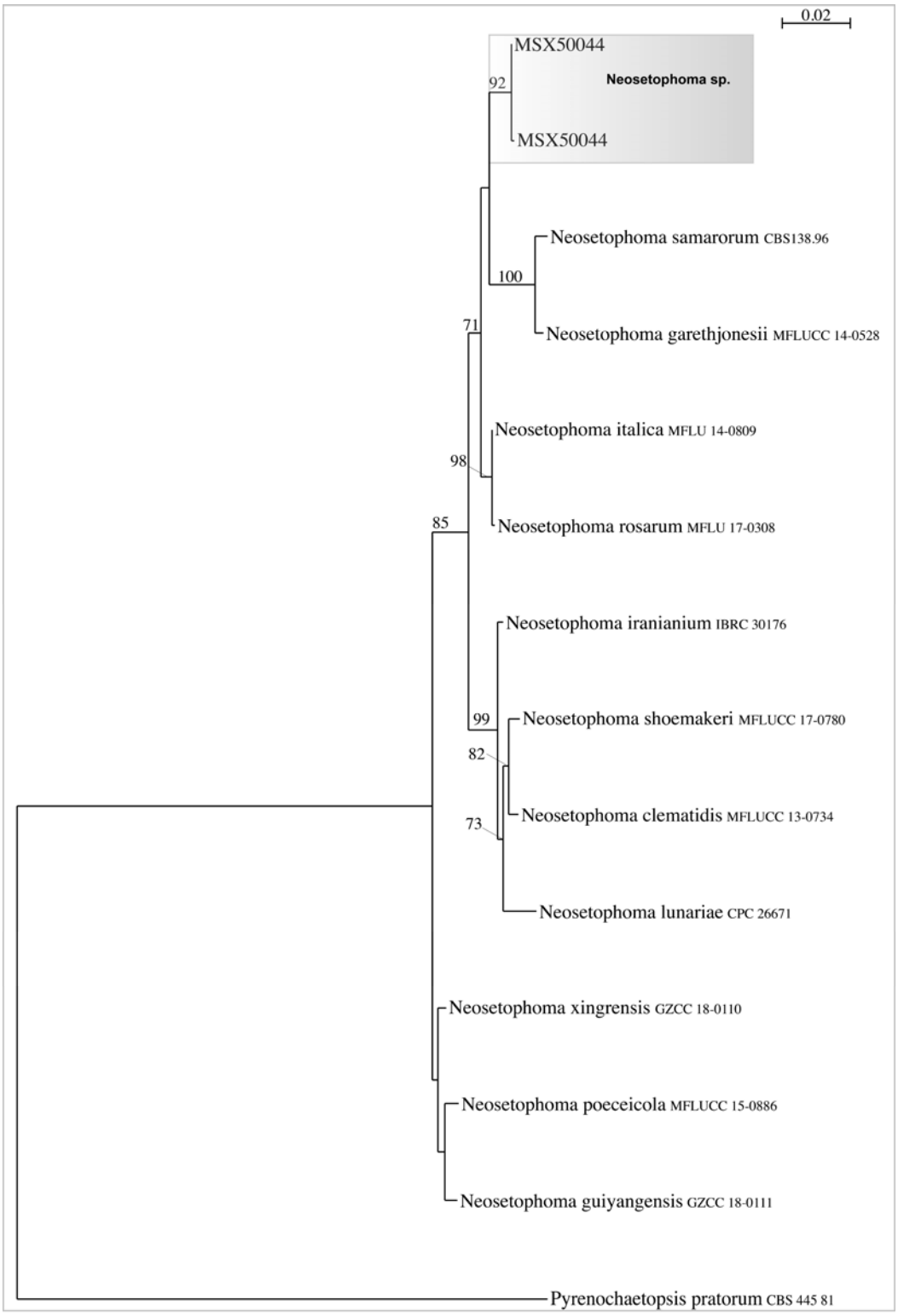

Figure S38. Phylogram of the most likely tree (-lnL = 2946.62) from a PHYML analysis of 14 taxa based on combined ITS and LSU sequence data (1416 bp). Numbers refer to PHYML bootstrap support values ≥ 70% based on 1000 replicates. Strain MSX50044 is identified as *Neosetophoma* sp. (Box highlighted in gray) as it groups with other *Neosetophoma* spp., including type strain *N. samarorum* (CBS 138.96). Bar indicates nucleotide substitutions per site.

REFERENCES

(1) de Gruyter, J.; Woudenberg, J. H. C.; Aveskamp, M. M.; Verkley, G. J. M.; Groenewald, J. Z.; Crous, P. W. *Mycologia* **2010**, *102*, 1066.

(2) Wijayawardene, N. N., Hyde, K.D., Rajeshkumar, K.C. et al *Fungal Divers.* **2017**, *86*, 1.

(3) Karunarathna, A.; Papizadeh, M.; Senanayake, I. C.; Jeewon, R.; Phookamsak, R.; Goonasekara, I. D.; Wanasinghe, D. N.; Wijayawardene, N. N.; Amoozegar, M. A.; Shahzadeh Fazeli, S. A.; Camporessi, E. *Mycosphere* **2017**, *8*, 1818.

(4) Hernández-Restrepo, M.; Schumacher, R. K.; Wingfield, M. J.; Ahmad, I.; Lei, C.; Duong, T. A.; Edwards, J.; Gené, J.; Groenewald, J. Z.; Jabeen, S.; Khalid, A. N.; Lombard, L.; Madrid, H.; Marin-Felix, Y.; Marincowitz, S.; Miller, A. N.; Rajeshkumar, K. C.; Rashid, A.; Sarwar, S.; Stchigel, A. M.; Taylor, P. W. J.; Nan, Z.; Crous, P. W. *Sydowia* **2016**, *68*, 193.

(5) Hyde KD, C. N., Norphanphoun C, Boonmee S, et al. *Mycosphere* **2018**, *9*, 271.

(6) Raja, H. A.; Kaur, A.; El-Elimat, T.; Figueroa, M.; Kumar, R.; Deep, G.; Agarwal, R.; Faeth, S. H.; Cech, N. B.; Oberlies, N. H. *Mycology* **2015**, *6*, 8.

(7) Raja, H. A.; Oberlies, N. H.; El-Elimat, T.; Miller, A. N.; Zelski, S. E.; Shearer, C. A. *Mycoscience* **2013**, *54*, 353.

(8) Raja, H. A.; Oberlies, N. H.; Figueroa, M.; Tanaka, K.; Hirayama, K.; Hashimoto, A.; Miller, A. N.; Zelski, S. E.; Shearer, C. A. *Mycologia* **2013**, *105*, 959.

(9) El-Elimat, T.; Figueroa, M.; Raja, H. A.; Graf, T. N.; Adcock, A. F.; Kroll, D. J.; Day, C. S.; Wani, M. C.; Pearce, C. J.; Oberlies, N. H. *Journal of Natural Products* **2013**, *76*, 382.

(10) Raja, H. A.; Miller, A. N.; Pearce, C. J.; Oberlies, N. H. *J. Nat. Prod.* **2017**, *80*, 756.

(11) de Gruyter, J.; Woudenberg, J. H. C.; Aveskamp, M. M.; Verkley, G. J. M.; Groenewald, J. Z.; Crous, P. W. *Mycologia* **2010**, *102*, 1066.

(12) Liu, J.-K.; Hyde, K. D.; Jones, E. B. G.; Ariyawansa, H. A.; Bhat, D. J.; Boonmee, S.; Maharachchikumbura, S. S. N.; McKenzie, E. H. C.; Phookamsak, R.; Phukhamsakda, C.; Shenoy, B. D.; Abdel-Wahab, M. A.; Buyck, B.; Chen, J.; Chethana, K. W. T.; Singtripop, C.; Dai, D.-Q.; Dai, Y. C.; Daranagama, D. A.; Dissanayake, A. J.; Doilom, M.; D'souza, M. J.; Fan, X. L.; Goonasekara, I. D.; Hirayama, K.; Hongsanan, S.; Jayasiri, S. C.; Jayawardena, R. S.; Karunarathna, S. C.; Li, W.-J.; Mapook, A.; Norphanphoun, C.; Pang, K.-L.; Perera, R. H.; Peršoh, D.; Pinruan, U.; Senanayake, I. C.; Somrithipol, S.; Suetrong, S.; Tanaka, K.; Thambugala, K. M.; Tian, Q.; Tibpromma, S.; Udayanga, D.; Wijayawardene, N. N.; Wanasinghe, D.; Wisitrassameewong, K.; Zeng, X. Y.; Abdel-Aziz, F. A.; Adamčík, S.; Bahkali, A. H.; Boonyuen, N.; Bulgakov, T.; Callac, P.; Chomnunti, P.; Greiner, K.; Hashimoto, A.; Hofstetter, V.; Kang, J.-C.; Lewis, D.; Li, X.-H.; Liu, X. Z.; Liu, Z.-Y.; Matsumura, M.; Mortimer, P. E.; Rambold, G.; Randrianjohany, E.; Sato, G.; Sri-Indrasutdhi, V.; Tian, C. M.; Verbeken, A.; von Brackel, W.; Wang, Y.; Wen, T. C.; Xu, J.-C.; Yan, J.-Y.; Zhao, R. L.; Camporesi, E. *Fungal Divers.* **2015**, *72*, 1.

(13) Aveskamp, M. M.; Verkley, G. J. M.; de Gruyter, J.; Murace, M. A.; Perelló, A.; Woudenberg, J. H. C.; Groenewald, J. Z.; Crous, P. W. *Mycologia* **2009**, *101*, 363.

(14) Ayers, S.; Graf, T. N.; Adcock, A. F.; Kroll, D. J.; Matthew, S.; Carcache de Blanco, E. J.; Shen, Q.; Swanson, S. M.; Wani, M. C.; Pearce, C. J.; Oberlies, N. H. *J. Nat. Prod.* **2011**, *74*, 1126.

(15) El-Elimat, T.; Figueroa, M.; Raja, H. A.; Graf, T. N.; Adcock, A. F.; Kroll, D. J.; Day, C. S.; Wani, M. C.; Pearce, C. J.; Oberlies, N. H. *J. Nat. Prod.* **2013**, *76*, 382.

(16) Figueroa, M.; Graf, T. N.; Ayers, S.; Adcock, A. F.; Kroll, D. J.; Yang, J.; Swanson, S. M.; Munoz-Acuna, U.; Carcache de Blanco, E. J.; Agrawal, R.; Wani, M. C.; Darveaux, B. A.; Pearce, C. J.; Oberlies, N. H. *J. Antibiot.* **2012**, *65*, 559.

(17) Sheldrick, G. *Acta Crystallographica Section C* **2015**, *71*, 3.

(18) Dolomanov, O. V.; Bourhis, L. J.; Gildea, R. J.; Howard, J. A. K.; Puschmann, H. *J. Appl. Crystallogr.* **2009**, *42*, 339.

(19) Westrip, S. *J. Appl. Crystallogr.* **2010**, *43*, 920.

(20) Carney, D. N.; Gazdar, A. F.; Bunn, P. A., Jr.; Guccion, J. G. *Stem Cells* **1982**, *1*, 149.

(21) Alali, F. Q.; El-Elimat, T.; Li, C.; Qandil, A.; Alkofahi, A.; Tawaha, K.; Burgess, J. P.; Nakanishi, Y.; Kroll, D. J.; Navarro, H. A.; Falkinham, J. O.; Wani, M. C.; Oberlies, N. H. *J. Nat. Prod.* **2005**, *68*, 173.

(22) Li, C.; Lee, D.; Graf, T. N.; Phifer, S. S.; Nakanishi, Y.; Riswan, S.; Setyowati, F. M.; Saribi, A. M.; Soejarto, D. D.; Farnsworth, N. R.; Falkinham, J. O., 3rd; Kroll, D. J.; Kinghorn, A. D.; Wani, M. C.; Oberlies, N. H. *J. Nat. Prod.* **2009**, *72*, 1949.